6-21-2010

# Particle-γ Spectroscopy of the (p,d-γ)$^{155}$Gd Reaction: Neutron Single-quasiparticle States at N=91

J. M. Allmond

C. W. Beausang
*University of Richmond*, cbeausan@richmond.edu

J. O. Rasmussen

T. J. Ross

M. S. Basunia

***See next page for additional authors***



## Recommended Citation

Allmond, J., C. Beausang, J. Rasmussen, T. Ross, M. Basunia, L. Bernstein, D. Bleuel, W. Brooks, N. Brown, J. Burke, B. Darakchieva, K. Dudziak, K. Evans, P. Fallon, H. Jeppesen, J. Leblanc, S. Lesher, M. McMahan, D. Meyer, L. Phair, N. Scielzo, S. Stroberg, and M. Wiedeking. "Particle-γ Spectroscopy of the ($p$,$d$-γ)$^{155}$Gd Reaction: Neutron Single-quasiparticle States at $N$=91." *Physical Review C* 81, no. 6 (June 21, 2010): 064316: 1 - 64316: 17. doi:10.1103/PhysRevC.81.064316.

**Authors**
J. M. Allmond, C. W. Beausang, J. O. Rasmussen, T. J. Ross, M. S. Basunia, L. A. Bernstein, D. L. Bleuel, W. Brooks, N. Brown, J. T. Burke, B. Darakchieva, K. Dudziak, K. E. Evans, P. Fallon, H. B. Jeppesen, J. LeBlanc, S. R. Lesher, M. A. McMahan, D. A. Meyer, L. Phair, N. D. Scielzo, S. R. Stroberg, and M. Wiedeking

# Particle-$\gamma$ spectroscopy of the $(p, d\text{-}\gamma)^{155}$Gd reaction: Neutron single-quasiparticle states at $N = 91$

J. M. Allmond,[1,*] C. W. Beausang,[1] J. O. Rasmussen,[2] T. J. Ross,[1] M. S. Basunia,[2] L. A. Bernstein,[3] D. L. Bleuel,[3] W. Brooks,[1] N. Brown,[4,†] J. T. Burke,[3] B. K. Darakchieva,[1] K. R. Dudziak,[5] K. E. Evans,[6] P. Fallon,[2] H. B. Jeppesen,[2] J. D. LeBlanc,[5] S. R. Lesher,[3,‡] M. A. McMahan,[2] D. A. Meyer,[5] L. Phair,[2] N. D. Scielzo,[3] S. R. Stroberg,[6] and M. Wiedeking[3]

[1]*Department of Physics, University of Richmond, Virginia 23173, USA*
[2]*Nuclear Science Division, Lawrence Berkeley National Laboratory, Berkeley, California 94720, USA*
[3]*Lawrence Livermore National Laboratory, Livermore, California 94551, USA*
[4]*School of Physics, Georgia Institute of Technology, Atlanta, Georgia 30332, USA*
[5]*Department of Physics, Rhodes College, Memphis, Tennessee 38112, USA*
[6]*Department of Nuclear Engineering, University of California, Berkeley, California 94720, USA*

(Received 22 April 2010; published 21 June 2010)

A segmented Si telescope and HPGe array is used to study the $^{156}$Gd$(p, d\text{-}\gamma)^{155}$Gd direct reaction by $d$-$\gamma$ and $d$-$\gamma$-$\gamma$ coincidence measurements using 25-MeV protons. The present investigation is the first time that this $N = 91$ nucleus and the $N = 90$ region—which is known for a rapid change from vibrational to rotational character, several low-lying $0^+$ states in the even-even nuclei, and large Coriolis ($\Delta\Omega = 1$) plus $\Delta N = 2$ mixing in the even-odd nuclei—have been studied by particle-$\gamma$ coincidence following a direct reaction with light ions. Gamma-ray energies and branches, excitation energies, angular distributions, and cross sections are measured for states directly populated in the $(p, d)$ reaction. A new low-energy doublet state at 592.46 keV (previously associated with the $K = 0 \otimes \frac{3}{2}^-[521]$ bandhead) and several new $\gamma$-ray transitions (particularly for states with excitation energies $>1$ MeV) are presented. Most notably, the previous $\nu\, \frac{7}{2}^+[404]$ systematics at and around the $N = 90$ transition region are brought into question and reassigned as $\nu\, \frac{5}{2}^+[402]$. This reassignment makes the $\nu\, \frac{1}{2}^+[400]$, $\nu\, \frac{3}{2}^+[402]$, and $\nu\, \frac{5}{2}^+[402]$ orbitals, which originate from the $3s_{1/2}$, $2d_{3/2}$, and $2d_{5/2}$ spherical states, respectively, responsible for the three largest cross sections to positive-parity states in the $(p, d)^{155}$Gd direct reaction. These three steeply upsloping orbitals undergo $\Delta N = 2$ mixing with their $N = 6$ orbital partners, which are oppositely sloped with respect to deformation. The presence of these steeply sloped and crossing orbitals near the Fermi surface could weaken the monopole pairing strength and increase the quadrupole pairing strength of neighboring even-even nuclei, which would bring $\nu$ 2p-2h $0^+$ states below $2\Delta$. Indeed, this could account for a large number of the low-lying $0^+$ states populated in the $(p, t)^{154}$Gd direct reaction.

DOI: 10.1103/PhysRevC.81.064316 PACS number(s): 24.50.+g, 23.20.Lv

## I. INTRODUCTION

The rare-earth nucleus $^{155}$Gd ($Z = 64$, $N = 91$, $\delta \sim 0.3$) is positioned near the center of a mass region that is known for a rapid change from vibrational to rotational character [1–3]. Although it has been experimentally studied by many groups, the present study is the first time $^{155}$Gd and the $N = 90$ transition region have been studied by particle-$\gamma$ coincidence following a direct reaction with light ions. The $^{156}$Gd$(p, d\text{-}\gamma)^{155}$Gd direct reaction is employed in the present study.

The adopted level scheme of $^{155}$Gd [4] is based primarily on the results of the following studies: $(d, p)$ and $(d, t)$ by Tjøm and Elbek [5], $^{155}$Eu $\beta^-$ decay by Foin *et al.* [6] and Meyer and Meadows [7], $(d, t)$ by Jaskola *et al.* [8], Coulex by Tveter and Herskind [9], $(\alpha, 3n)$ by Løvhøiden *et al.* [10], $(d, d')$ by Sterba *et al.* [11], $(^3$He, $\alpha)$ by Løvhøiden *et al.* [12], $(p, t)$ by Løvhøiden *et al.* [13], $^{155}$Tb electron capture by Meyer *et al.* [14], and $(d, t)$, $(d, p)$, and $(n, \gamma)$ by Schmidt *et al.* [15]. Although there are other $^{155}$Gd studies, only those relevant to the present study are listed; there are no previous $(p, d)^{155}$Gd studies reported in the literature.

We note that these previous experimental studies of $^{155}$Gd are primarily from the late 1960s and early 1970s with the exception of the $(d, t)$, $(d, p)$, and $(n, \gamma)$ study by Schmidt *et al.* [15] in 1986. Indeed, there have been few studies (particularly nucleon transfer studies) in recent years for the odd-mass nuclei in the $N = 91$ region. Two of the most recent nucleon transfer studies for $N = 91$ include $(p, d)^{153}$Sm by Blasi *et al.* [16] and $(^3$He, $\alpha)^{153}$Sm by Gollwitzer *et al.* [17]. However, although there has not been much activity lately for the odd-mass nuclei near $N = 91$, there has been for the even-even nuclei at $N = 90$ (i.e., at the center of the transitional region [1–3]), which includes, in part, the following experimental studies: $^{152}$Sm from the $\epsilon$ decay of $^{152}$Eu by Casten *et al.* [18] and Zamfir *et al.* [19], $^{152}$Sm from multistep Coulomb excitation and from the $\beta$ decay of $^{152m,g}$Eu by Kulp *et al.* [20], $(n, n'\gamma)^{152}$Sm by Garrett *et al.* [21], $^{154}$Gd from the $\beta$ decay of $^{154}$Eu and $^{154g,m1,m2}$Tb by Kulp *et al.* [22], and $(p, t)^{154}$Gd by Meyer *et al.* [23]. Indeed, the entire $N = 90$ transition region could benefit from nucleon-transfer studies using the particle-$\gamma$ coincidence technique presented in the following study.

*Present address: Joint Institute for Heavy Ion Research, Oak Ridge National Laboratory, Oak Ridge, Tennessee 37831, USA.
†Present address: Department of Physics/TUNL, Duke University, Durham, North Carolina 27708, USA.
‡Present address: Department of Physics, University of Wisconsin, La Crosse, Wisconsin 54601, USA.

 

Nilsson model [24] calculations with Coriolis ($\Delta\Omega = 1$) and $\Delta N = 2$ mixing [5,10,25–28] have been very successful in describing the general features of the low-lying states in $^{155}$Gd. However, many of the adopted Nilsson assignments in $^{155}$Gd [4] originate from the 1967 experimental and theoretical study of Tjøm and Elbek [5]. A broader scope of the rare-earth region is outlined in two 1969 review articles by Elbek and Tjøm [29] and, separately, by Bunker and Reich [30] (i.e., for neutron single-quasiparticle states of odd-mass nuclei). A general outcome of the studies is that the Nilsson model [24] correctly describes the rare-earth data (level energies, spins, and cross sections) when Coriolis ($\Delta\Omega = 1$) and $\Delta N = 2$ couplings are included. Interestingly, of all the rare-earth nuclei, one of the best-known cases of $\Delta N = 2$ mixing is between the $\nu\,\frac{3}{2}^+[651]$ and $\nu\,\frac{3}{2}^+[402]$ orbitals in $^{155}$Gd ($N = 91$) [5,28,30], which are steeply and oppositely sloped (with respect to deformation) near the Fermi surface.

Despite the success of the Nilsson model in describing the low-energy levels in $^{155}$Gd, there are discrepancies, inconsistencies, and failures between theory and experiment; this is particularly true at higher excitation energies, $E_x >$ 1 MeV, where data between particle and $\gamma$-ray experiments can be incorrectly associated owing to the larger level density. The present study uses particle-$\gamma$ coincidences from the $^{156}$Gd$(p, d\text{-}\gamma)^{155}$Gd direct reaction to associate states and $\gamma$-ray transitions in a more dependable manner. Furthermore, the particle-$\gamma$ coincidences are used to make spin assignments by a combined use of angular distributions and $\gamma$-decay paths, which often can unambiguously assign the transferred angular momentum, $L$, and spin, $J^\pi$.

## II. EXPERIMENT

The experiment was carried out at the 88-Inch Cyclotron of the Lawrence Berkeley National Laboratory. A 25-MeV (∼2.5-enA) proton beam was used to study the $^{156}$Gd$(p, d\text{-}\gamma)^{155}$Gd direct reaction and subsequent $\gamma$ emission. The $^{156}$Gd target was self-supporting and 825 $\mu$g/cm$^2$ thick.

Particle data were taken with the Silicon Telescope Array for Reaction Studies (STARS, [31,32]) consisting of two large-area, double-sided, annular Si detectors (segmented into rings, $\theta$, and sectors, $\phi$) configured in a $\Delta E$-$E$ (140–1000 $\mu$m) telescope array at forward angles $\theta_{\text{for}} \approx 33^\circ$–$51^\circ$ with respect to and symmetric about the beam axis (i.e., in azimuth, $\phi$). Coincident $\gamma$-ray data were collected with the Livermore-Berkeley Array for Collaborative Experiments (LIBERACE, [32]), consisting of six Compton-suppressed HPGe clover detectors [33] and one LEPS detector, arranged in 45° increments within a single plane parallel to the beam axis, and one clover perpendicular to this plane and 90° to the beam axis. Figure 1 shows a schematic of the $^{156}$Gd target and detector arrangement used in the present study.

The experimental trigger required at least one of the following events: particle (i.e., a light ion detected in both Si detectors of the Si-telescope array), particle-$\gamma$, or $\gamma$-$\gamma$. Timing information was provided with each trigger relative to the cyclotron rf frequency (∼91 ns between pulses) to differentiate between prompt and nonprompt events.

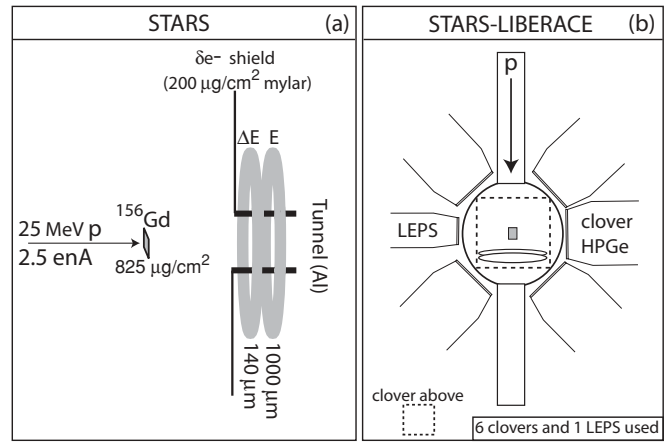


FIG. 1. (a) A schematic of the STARS and $^{156}$Gd target arrangement used in the present study. (b) A schematic of the STARS-LIBERACE array. See text for details.

Selectivity to the direct-reaction channel was achieved by the differential energy loss of the different light ions in the Si telescope (see Fig. 2). Additionally, a ray-trace (i.e., a geometric trace back to the target using the segmentation of the annular detectors) vetoed scattered beam events from the data set. Each Si detector was corrected for cross-talk (induced noise) and legitimate firing of adjacent rings (i.e., the ions can physically traverse more than one ring in a single Si detector).

The in-beam energy resolution of the Si telescope was FWHM ∼370 keV and was limited by kinematic broadening, intrinsic resolution of the Si detectors, and pileup events. The energy calibration of the Si-telescope array was set by the following sources: (1) prerun and postrun calibrations with a $^{226}$Ra $\alpha$ source, (2) direct population of known states in the $(p, d)^{155}$Gd and $(p, t)^{154}$Gd direct reactions, and (3) onset of neutron evaporation in the $(p, dn)$ channel at the neutron evaporation threshold, $S_n = 6.432$ MeV. The total clover add-back resolution [33] at 1000 keV was FWHM ∼ 3 keV and the add-back singles peak efficiency at 1000 keV was $\epsilon_{\gamma\text{-singles}} \sim 1.3\%$ (determined from a $^{152}$Eu $\gamma$-ray calibration source).

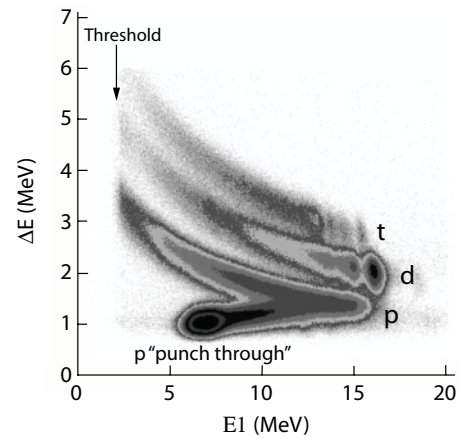


FIG. 2. A particle-identification plot showing the protons, deuterons, and tritons detected by the Si-telescope array of STARS.

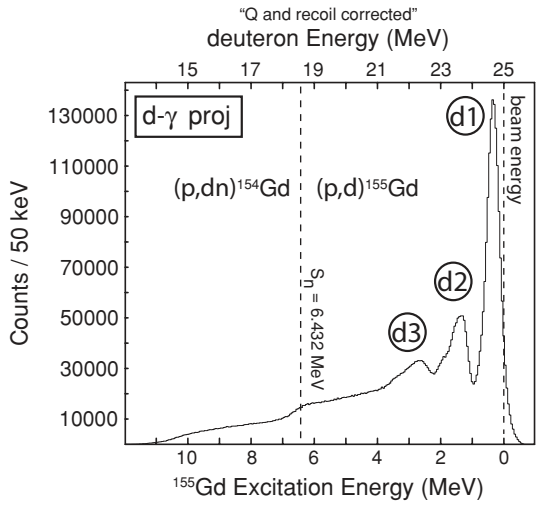


FIG. 3. The deuteron projection of the prompt $d$-$\gamma$ coincidence matrix.

During the course of the experiment, $5 \times 10^6$ $d$-$\gamma$ and $7 \times 10^5$ $d$-$\gamma$-$\gamma$ events were recorded over 3 days. The present study organizes the data primarily in three ways:

(i) $d$-$\gamma$ coincidences,
(ii) $d$-$\gamma$-$\gamma$ triple coincidences (i.e., a deuteron-gated $\gamma$-$\gamma$ matrix), and
(iii) $d$-$\theta_d$-$\gamma$ coincidences (for angular distributions).

## III. PARTICLE-$\gamma$ SPECTROSCOPY OF $^{156}$Gd$(p, d\gamma)^{155}$Gd

The total $\gamma$-gated deuteron spectrum from $^{156}$Gd$(p, d$-$\gamma)^{155}$Gd is shown in Fig. 3. Because neutrons were not measured in the experiment, this deuteron spectrum contains events from the $(p, dn\gamma)^{154}$Gd reaction channel as well, which can be seen for $E_x > S_n = 6.432$ MeV. However, by selecting only the deuterons that correspond to $E_x < S_n$, the coincident $\gamma$ rays from $^{154}$Gd can be eliminated. Likewise, by selecting only the deuterons that correspond to $E_x > S_n$, the coincident $^{155}$Gd $\gamma$ rays can be "mostly" eliminated [i.e., the $(p, d\gamma)$ cross section is nonzero even for $E_x > S_n$]. Overall, the deuteron spectrum in Fig. 3 is dominated by three large quasidiscrete features labeled as d1, d2, and d3. As will be shown later, the multiple discrete states that make up these ensembles can be individually selected with coincident discrete $\gamma$ rays.

A gate on a discrete $\gamma$-ray transition from $(p, d$-$\gamma)^{155}$Gd typically shows two features in the coincident deuteron spectrum: (1) the deuterons, by excitation energy, that correspond to the direct population of a state from which the $\gamma$ ray originated and (2) the deuterons that correspond to other higher lying states, also directly populated in the reaction, which subsequently decay to the level selected by the $\gamma$ coincidence. An immediate consequence of these two features is that $\gamma$ transitions that depopulate the same state will show identical coincident deuteron spectra (within statistical uncertainty). Furthermore, $\gamma$-ray doublets from different reaction channels [e.g., $(p, d\gamma)$ and $(p, dn\gamma)$] are clearly distinguishable from the large separation in measured deuteron energy. Gamma-ray doublets from the same reaction channel may or may not be well separated in coincident deuteron energy; if not, the $d$-$\gamma$-$\gamma$ coincidences can generally resolve it.

The focus of this $(p, d$-$\gamma)^{155}$Gd study is on the excitation energy region from 0 to $\sim 4$ MeV corresponding to the quasidiscrete features (d1, d2, and d3) in the deuteron total projection (Fig. 3). A new state (doublet) with two $\gamma$ branches is found in the d1 region. Discrete $\gamma$ rays depopulating levels previously known from magnetic spectrometer work are found for the first time in the d2 region. No discrete $\gamma$ peaks are found in coincidence with the high-energy d3 feature. However, there is a slight "hump" in the $\gamma$ continuum for $1.5 \geqslant E_\gamma \geqslant 3$ MeV, which is correlated to the d3 feature (and vice versa) in Fig. 3.

A low-lying, $E_x < 500$-keV, partial level scheme of $^{155}$Gd, adopted from *Nuclear Data Sheets* (NDS) [4], is shown in Fig. 4, which illustrates the levels to which the states of interest in this study decay. Because there are many low-energy (<60 keV) and/or converted transitions for this region of the level scheme, which are not observed in this experiment (i.e., low detection efficiency for $E_\gamma < 60$ keV and no conversion

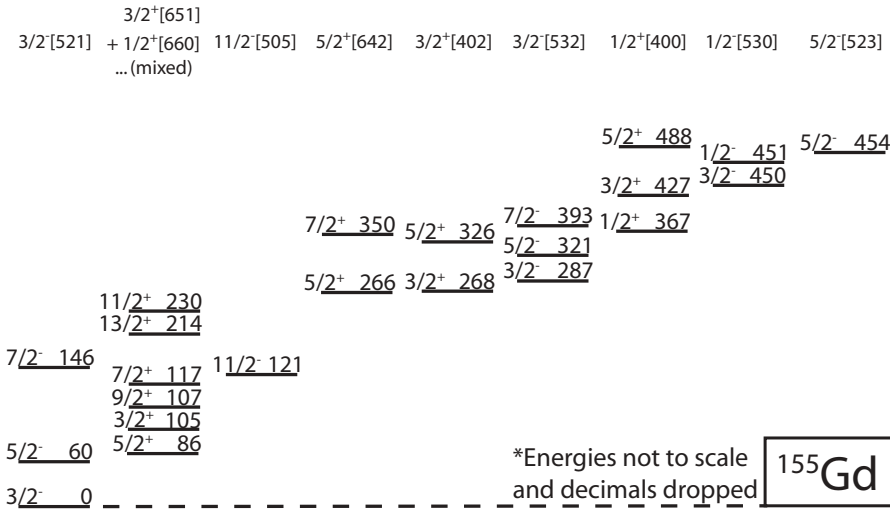


FIG. 4. A low-lying, $E_x < 500$-keV, partial level scheme of $^{155}$Gd, adopted from *Nuclear Data Sheets* (NDS) [4], illustrating the levels to which the states of interest in this study decay. The levels are labeled by their excitation energy in keV (decimals dropped) and spin/parity $J^\pi$; the bands are organized and labeled by their adopted Nilsson assignment.

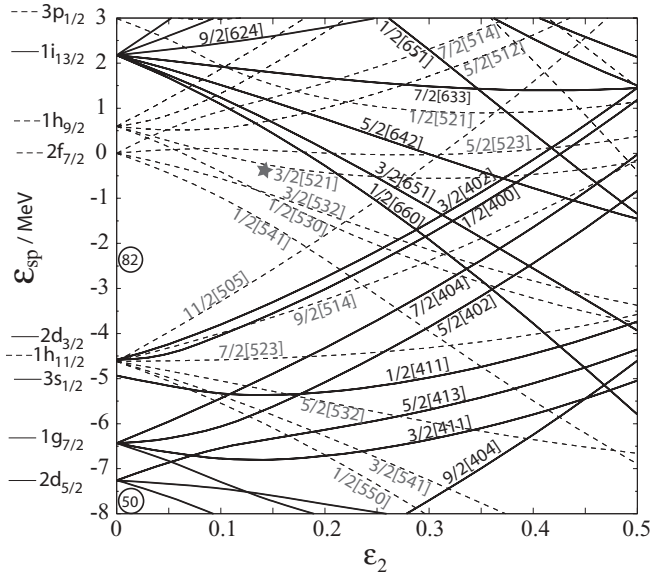


FIG. 5. The Nilsson diagram centered near the $N = 91$ region. The ground-state orbital for $^{155}$Gd, $\frac{3}{2}^-[521]$, is marked by a star. The diagram was generated with the tilted-axis cranking code [34].

electron detector), the present study is partially dependent upon the data in NDS [4] and so the level energies, spins, $\gamma$-ray energies, branching ratios, and conversion-electron coefficients are adopted [4] for $E_x < 500$ keV; no inconsistencies are found in this region between our data and the data in NDS [4].

The Nilsson diagram shown in Fig. 5 illustrates the relative positions of the "adopted" (cf. Nilsson assignments and bandheads in Fig. 4) and neighboring neutron single-particle orbitals as a function of deformation, $\epsilon_2 = \delta + (1/6)\delta^2 + (5/18)\delta^3 + (37/216)\delta^4 + \cdots$. The $(p,d)^{155}$Gd single-neutron transfer (pickup) reaction is expected to "pluck" neutrons from orbitals lying close to or below the $N = 91$ neutron Fermi surface. The theory on this is partially outlined in the following.

The particle-$\gamma$ double-differential cross section for a direct reaction followed by $\gamma$ decay is [35]

$$\frac{d^2\sigma}{d\Omega_d d\Omega_\gamma} = \frac{1}{4\pi}\frac{\Gamma_f}{\Gamma}W(d\Omega_\gamma)\frac{d\sigma}{d\Omega_d}, \tag{1}$$

where $\Gamma_f$ is the fractional decay width of the total decay width, $\Gamma$, and $W(d\Omega_\gamma)$ is the particle-$\gamma$ anisotropy. The particle single-differential cross section can be written in terms of the double-differential cross section as

$$\frac{d\sigma}{d\Omega_d} = \frac{\Gamma}{\Gamma_f}\frac{4\pi}{W(d\Omega_\gamma)}\frac{d^2\sigma}{d\Omega_d d\Omega_\gamma}. \tag{2}$$

However, without complete knowledge of all decay paths, $\Gamma$, only a lower limit of the single-differential cross section can be determined.

The theoretical differential cross section for a pickup reaction (single-nucleon transfer) from an even-even target to a state of spin $I = j$ is [36]

$$\frac{d\sigma}{d\Omega_d} = 2(C_{jl}\,V)^2 N\sigma_l(\theta), \tag{3}$$

for unmixed Nilsson configurations, and

$$\frac{d\sigma}{d\Omega_d} = 2\left(\sum_i C^i_{jl}\,a_i\,V_i\right)^2 N\sigma_l(\theta), \tag{4}$$

for mixed configurations, where $C^i_{jl}$ is the Nilsson expansion coefficient of the one-quasiparticle Nilsson state, orbital $i$, in a spherical basis, $a_i$ is the mixing amplitude for orbital $i$ (e.g., from Coriolis, $\Delta\Omega = 1$, and $\Delta N = 2$ mixing), $V_i^2$ is the occupation probability for orbital $i$, $N$ is a normalization factor dependent upon the type of reaction used, and $\sigma_l(\theta)$ is the distorted-wave Born approximation (DWBA) cross section. The $C_{jl}$ coefficients ($\leqslant 1$) have been tabulated by Chi [37] for several deformations, $\delta$.

The occupation probability, $V^2$, can be expressed as

$$V^2 = \frac{1}{2}\left(1 - \frac{\epsilon_{\rm sp} - \lambda_f}{\epsilon_{\rm qp}}\right), \tag{5}$$

where $\epsilon_{\rm qp}$ is the quasiparticle energy,

$$\epsilon_{\rm qp} = \sqrt{(\epsilon_{\rm sp} - \lambda_f)^2 + \Delta^2}, \tag{6}$$

$\epsilon_{\rm sp}$ is the single-particle energy, $\lambda_f$ is the Fermi energy, and $\Delta$ is half the pair gap. The excitation energy is the difference in quasiparticle energy from that of the excited and ground state,

$$E_x \approx \sqrt{(\epsilon_{\rm sp} - \lambda_f)^2 + \Delta^2} - \Delta. \tag{7}$$

The emptiness probability, $U^2$, is simply

$$U^2 = 1 - V^2. \tag{8}$$

Therefore, the occupation probability goes from 50% to 100% and the emptiness probability goes from 50% to 0% for $E_x \geqslant 0$ and $\epsilon_{\rm sp} < \lambda_f$ (with the reverse being true for $\epsilon_{\rm sp} > \lambda_f$). However, it is important to note that although the occupation probability, $V^2$, goes to unity for an orbital far below the Fermi surface, $\lambda_f$, the DWBA cross section, $\sigma_l(\theta)$, can significantly decrease owing to a kinematics or $Q$-window "mismatch."

The pickup cross section for a given angular momentum transfer, $L$, from an orbital near the Fermi surface is, to first order, dictated by the $C_{jl}$ expansion coefficient. In general, the $C_{jl}$ coefficient is largest when the transferred angular momentum is equal to (or nearly equal to) the spin of the spherical parent of the populated Nilsson orbital. For example, the $(C_{jl})^2$ coefficients for the $\frac{1}{2}^+[400]$ ($L = 0$) and $\frac{3}{2}^+[402]$ ($L = 2$) Nilsson orbitals, which originate from the $3s_{1/2}$ and $2d_{3/2}$ spherical states, respectively, have values of 0.606 and 0.850 [37], respectively. In contrast, the $(C_{jl})^2$ coefficients for the $\frac{1}{2}^+[660]$ ($L = 0$) and $\frac{3}{2}^+[651]$ ($L = 2$) Nilsson orbitals, which originate from the $1i_{13/2}$ spherical state, have values of 0.006 and 0.001 [37], respectively (i.e., two and three orders of magnitude smaller). It is important to note, however, that mixing could reduce or increase these differences. Using the $C_{jl}$ expansion coefficients of Chi [37] as a qualitative guide, one finds that the largest $L = 0$ cross section in $(p,d)^{155}$Gd is expected to be from the $\frac{1}{2}^+[400]$ orbital. Likewise, the largest $L = 2$ cross section is expected to be from the $\frac{3}{2}^+[402]$ orbital (cf. the low-lying level scheme in Fig. 4 and the orbitals in Fig. 5).

### A. Examples with the two largest cross sections: $\nu\ \frac{1}{2}^+[400]$ and $\nu\ \frac{3}{2}^+[402]$

The two largest cross sections in the present $(p, d\text{-}\gamma)^{155}$Gd study are to states at excitations of $367.66 \pm 0.10$ and $268.67 \pm 0.10$ keV (cf. $367.6340 \pm 0.0008$ and $268.6233 \pm 0.0007$ keV in NDS [4]). These two levels also represent the two largest cross sections in previous $(d, t)$ studies [5,8,15] (single-neutron pickup reactions). All three $(d, t)^{155}$Gd studies report direct population of the 367- and 268-keV levels by $L = 0$ and $L = 2$ transfer and make Nilsson assignments of $\frac{1}{2}^+[400]$ and $\frac{3}{2}^+[402]$, respectively (adopted by NDS [4]), which is consistent with the expectations of the simplified theory presented here. The 367- and 268-keV levels are shown in Fig. 4 and the $\frac{1}{2}^+[400]$ and $\frac{3}{2}^+[402]$ orbitals are shown in Fig. 5. These two states are used to establish and illustrate the power (and limitation) of the particle-$\gamma$ coincidence technique before applying it to other states.

The 367-keV, $\frac{1}{2}^+[400]$, level is selected and observed in the present study by the decay of two $\gamma$-ray transitions: 262 and 281 keV [4]. Figure 6 shows the deuteron spectrum in coincidence with the 262-keV $\gamma$ ray. As can be seen, the deuteron spectrum is dominated by a single peak (whose width is consistent with the experimental resolution) at a measured excitation energy of $364 \pm 5$ keV, which is in excellent agreement with the previously known excitation energy of $367.6340 \pm 0.0008$ keV [4]. Alternatively, by gating on deuteron energies around 367 keV, the 262-keV $\gamma$ ray can be measured more precisely, $262.34 \pm 0.10$ keV (cf. $262.322 \pm 0.002$ keV in NDS [4]), because of an improved peak-to-total ratio (i.e., the deuteron gate reduces the background in the $\gamma$ spectrum, which enhances the $\gamma$-ray peak). However, where possible, deuteron and $\gamma$ gates on the $d$-$\gamma$-$\gamma$ coincidence data can provide an additional measure of the $\gamma$-ray energy.

A second $\gamma$-ray, the 281-keV transition, also depopulates the 367-keV level [4] and, indeed, the coincident deuteron spectrum is identical to that from the 262-keV $\gamma$ gate shown in Fig. 6. The measured excitation energy of the $\frac{1}{2}^+[400]$ state based on the deuteron peak in the 281-keV $\gamma$ gate is $374 \pm 6$ keV, which is consistent with the previously known excitation energy. By gating on the deuteron energies around 367 keV, the 281-keV $\gamma$-ray energy is determined to be $281.22 \pm 0.13$ keV (cf. $281.087 \pm 0.002$ keV in NDS [4]). The 262- and 281-keV $\gamma$ transitions are the only two $\gamma$ branches from the 367-keV state [4] that can be measured in the present study (i.e., the other transitions are doublets, weak branches, low-energy $\gamma$ rays with low detection efficiency, dominated by internal conversion, or some combination of these). The relative $\gamma$ branches are determined to be $I_\gamma = 100.0 \pm 1.6$ and $5.82 \pm 0.17$, respectively (cf. $100 \pm 10$ and $6.2 \pm 0.6$ in NDS [4]).

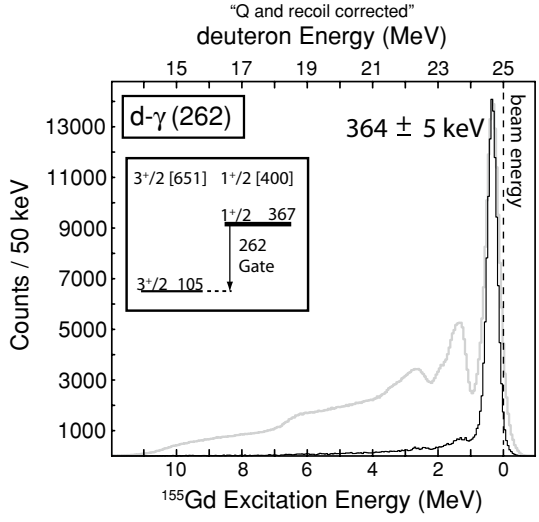


FIG. 6. The deuteron spectrum in coincidence with the 262-keV $\gamma$ ray (black) and the deuteron projection of the prompt $d$-$\gamma$ coincidence matrix (gray).

If the 367-keV, $\frac{1}{2}^+[400]$, level were new, the adopted excitation energy, based only on the $\gamma$-gated deuteron spectra, would be obtained by the linear-weighted average of measured excitation energies,

$$E_x^d\left(\tfrac{1}{2}^+[400]\right) = 367 \pm 7 \text{ keV}$$

(cf. $367.6340 \pm 0.0008$ keV in NDS [4]). However, in the present experiment, the excitation energy of a level can be very accurately determined (on the order of $\sim$0.1 keV) by use of deuteron-coincident $\gamma$ rays and knowledge of the low-lying decay scheme (cf. the "adopted" levels [4] in Fig. 4). That is, the excitation energy is given by $E_x = E_\gamma + E_f$; measuring multiple $\gamma$-ray decay paths of the same level give multiple measures of the initial level energy. An exercise is given in the following for the 367-keV, $\frac{1}{2}^+[400]$ example.

The final level energy, $E_f$, is determined by taking the difference between the measured excitation energy of the level from the $\gamma$-gated deuteron spectrum, $E_x^d$, and the energy of the gating $\gamma$ ray, $E_\gamma$. $E_f^{\text{NDS}}$ is then determined by comparing the measured value of $E_f = E_x^d - E_\gamma$ to the known level energies [4]. For instance, the $262.34 \pm 0.10$-keV $\gamma$-ray peak and $364 \pm 5$-keV deuteron excitation peak give a "final" level energy of $E_f = 102 \pm 5$ keV. There are two known levels within 5 keV of this: $105.3110 \pm 0.0006$ keV ($J^\pi = \frac{3}{2}^+$) and $107.5806 \pm 0.0010$ keV ($J^\pi = \frac{9}{2}^+$) [4]. The $281.22 \pm 0.13$-keV $\gamma$-ray peak and $374 \pm 6$-keV deuteron excitation peak give a "final" level energy of $E_f = 93 \pm 6$ keV. There is only one known level within 6 keV of this: $86.5468 \pm 0.0006$ keV ($J^\pi = \frac{5}{2}^+$) [4]. The resulting excitation energies are consistent and equal to $\sim 367$ keV only if 105 keV is chosen as the final level energy for the 262-keV $\gamma$ transition.

Typically, there are only a few low-lying levels in the level scheme within 5–12 keV of each other but, in case of the occasional ambiguity, a deuteron and $\gamma$ gate on $d$-$\gamma$-$\gamma$ coincidences can usually resolve the issue (although statistics are not always available for this consistency check). For example, the total deuteron-selected 262-keV $\gamma$ gate from $^{156}$Gd$(p, d\text{-}\gamma\text{-}\gamma)^{155}$Gd is shown in Fig. 7. The subsequent $\gamma$ decays are used to confirm the decay path [4] and excitation energy of the initial state; indeed, 105 keV is the final level energy of the 262-keV $\gamma$ transition.

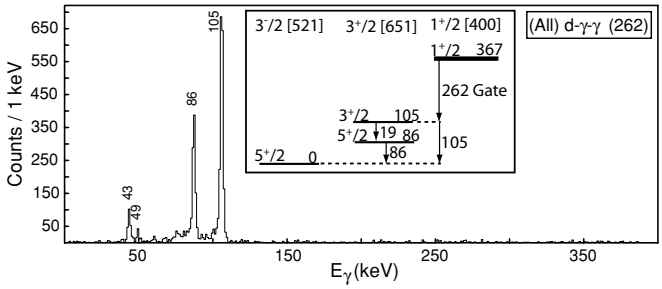


FIG. 7. The total deuteron-selected 262-keV $\gamma$ gate from $d$-$\gamma$-$\gamma$.

Using the $262.34 \pm 0.10$- and $281.22 \pm 0.13$-keV measured $\gamma$-ray energies and the known final level energies of $105.3110 \pm 0.0006$ and $86.5468 \pm 0.0006$ keV [4], respectively, one can determine the excitation energy of the $\frac{1}{2}^+[400]$ state to be (taking the linear-weighted average)

$$E_x\left(\tfrac{1}{2}^+[400]\right) = 367.66 \pm 0.10 \text{ keV}$$

(cf. $367.6340 \pm 0.0008$ keV in NDS [4]). Therefore, new level energies can be determined solely from particle-$\gamma$ coincidences to an accuracy determined by the energy of the $\gamma$ ray, $\sim$0.1 keV. This technique, especially in combination with $d$-$\gamma$-$\gamma$ coincidences, allows for accurate level-energy assignments. Furthermore, by having the approximate excitation energy from the deuterons, errors from "missing" $\gamma$-ray and/or converted transitions are avoided, which can be overlooked by the use of $\gamma$ rays alone.

The experimental and DWBA [38] angular distributions for the direct population of the 367-keV, $\frac{1}{2}^+[400]$, level are shown in Fig. 8 by a double gate on the 262-keV $\gamma$-ray peak and 367-keV deuteron peak via (367 keV)$d$-$\theta_d$-$\gamma$(262 keV); only the statistical errors are shown. The experimental angular distribution is most accurately described by $L = 0$ in the $\chi^2$ minimization (where $J = L \pm \frac{1}{2}$); the same result is obtained with a (367 keV)$d$-$\theta_d$-$\gamma$(281 keV) double gate. However, the $L = 1$ and 5 fits are also a reasonable match because of the limited angular coverage of our Si telescope, which spanned $\theta_{\text{for}} \approx 33^\circ$–$51^\circ$. The large $\chi^2$ value of the $L = 0$ fit reveals a breakdown in the DWBA ability to describe the data to the level of the experimental error. Nevertheless, the DWBA [38] theory proves useful in $L$-transfer assignments, especially when combined with the knowledge of the $\gamma$-decay paths.

The 268-keV, $\frac{3}{2}^+[402]$, level, which represents the second largest $(p, d)^{155}$Gd cross section, is selected and observed in the present study by the decay of two $\gamma$-ray transitions: 163 and 268 keV [4]. Figure 9 shows the deuteron spectrum in coincidence with the 163-keV $\gamma$ ray, which is dominated by a peak at a measured excitation energy of $275 \pm 6$ keV (cf. $268.6233 \pm 0.0007$ keV in NDS [4]). However, in this deuteron spectrum, a prominent second peak appears at a higher excitation energy of $1304 \pm 7$ keV. This peak indicates that another level is also directly populated in the reaction, which has a strong $\gamma$-ray branch to the 268-keV level. As mentioned earlier, the deuteron spectrum contains the entire "history" of $^{155}$Gd prior to the $\gamma$ decay of the selected level. Note that the history contains both discrete and continuum states; details of the second peak in Fig. 9 will be discussed later. The excitation energy of the 268-keV, $\frac{3}{2}^+[402]$, level is determined in the same manner as before for the 367-keV, $\frac{1}{2}^+[400]$, level (i.e., by use of two $\gamma$-ray transitions, $163.40 \pm 0.10$ and $268.64 \pm 0.10$ keV). The resulting excitation energy (by linear-weighted average) is

$$E_x^d\left(\tfrac{3}{2}^+[402]\right) = 274 \pm 5 \text{ keV}$$

from the deuterons and

$$E_x\left(\tfrac{3}{2}^+[402]\right) = 268.67 \pm 0.10 \text{ keV}$$

from the $\gamma$-ray energies (cf. $268.6233 \pm 0.0007$ keV in NDS [4]).

The experimental and DWBA [38] angular distributions for the direct population of the 268-keV, $\frac{3}{2}^+[402]$, level are shown in Fig. 10 by a (268 keV)$d$-$\theta_d$-$\gamma$(163 keV) double gate. Indeed, the experimental angular distribution is most accurately described by $L = 2$ in the $\chi^2$ minimization as expected; the same result is obtained with a (268 keV)$d$-$\theta_d$-$\gamma$(268 keV) double gate. Note that the $L = 2$ distribution is uniquely identifiable.

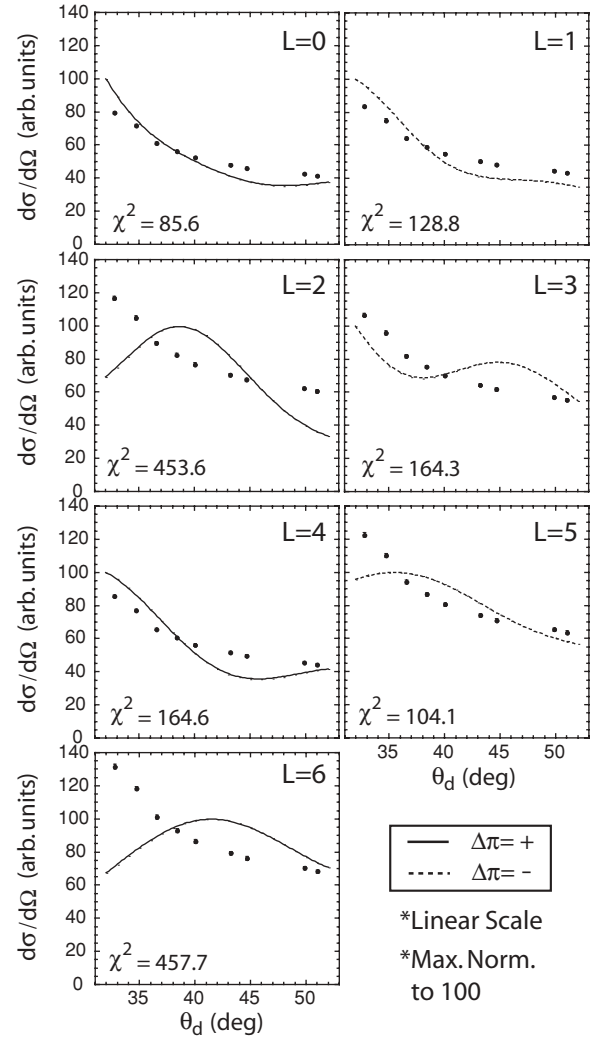


FIG. 8. An $L = 0$ example for the $\frac{1}{2}^+[400]$ state with a (367 keV)$d$-$\theta_d$-$\gamma$(262 keV) double gate.

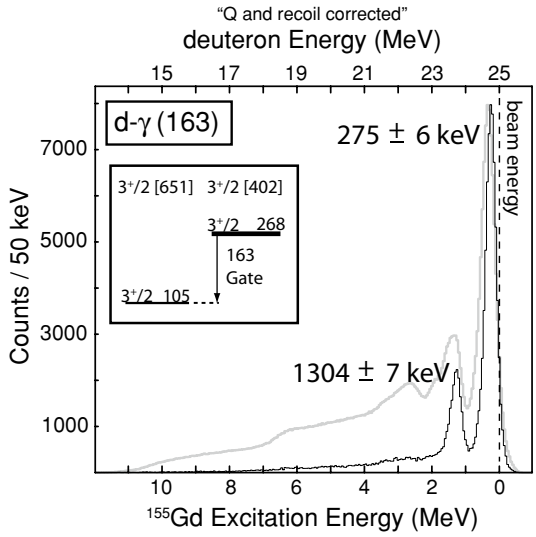


FIG. 9. The deuteron spectrum in coincidence with the 163-keV $\gamma$ ray (black).

The angular distributions were calculated with DWUCK4 [38] using the optical model parameters in Table I. The optical model parameters were chosen from the literature that best described the data with respect to the adopted $L$ values in NDS [4]. Within the angular range spanned by our Si-telescope array, the $L = 2$ distribution is especially unique in shape and will be important in future discussion. However, if more than one $L$ value matches the experimental (particle) angular distribution, the $\gamma$-decay path can often eliminate possible $L$ values and, further, assign a spin and parity, $J^\pi$, to the directly populated state. A summary of angular distribution shapes for each $L$ transfer value is given in Fig. 11; these are arbitrarily normalized to 100 at their maxima.

The experimental relative cross section for populating a state [cf. Eq. (2)] is determined from the $d$-$\gamma$ direct-population intensity (cf. the deuteron peak in Fig. 6) and the fractional decay width, $\Gamma_f$, of the level [4]. Therefore, the relative cross sections are

$$\sigma\left(\tfrac{1}{2}^+[400]\right) = 100.0 \pm 2.7 \text{ (arb. units)}$$

and

$$\sigma\left(\tfrac{3}{2}^+[402]\right) = 66.6 \pm 3.2 \text{ (arb. units)},$$

which are normalized to the largest cross section, $\frac{1}{2}^+[400]$, with an arbitrarily fixed value of 100. Now that the method has been established, new results are presented.

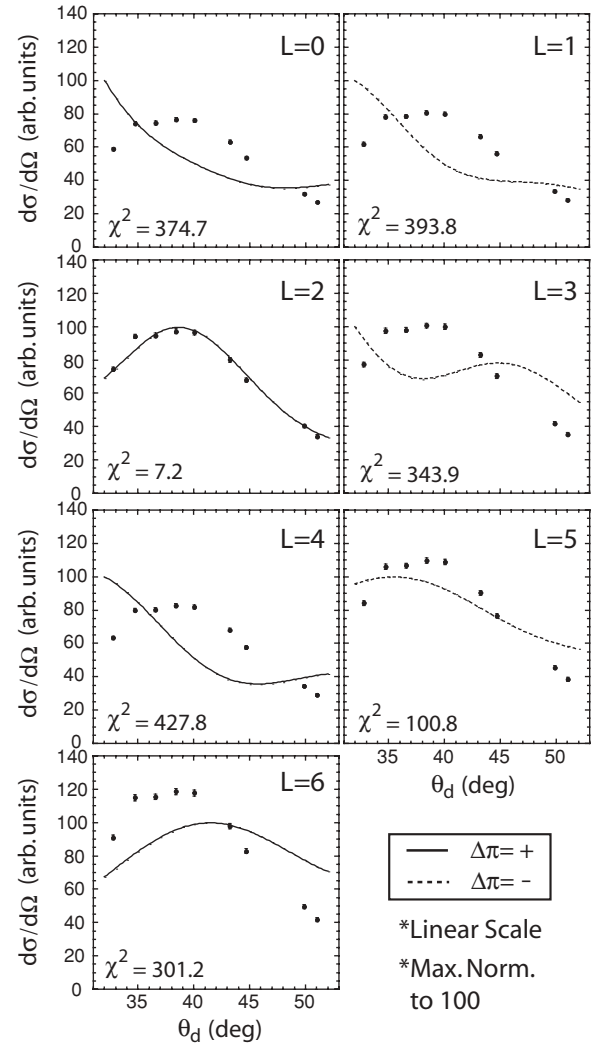


FIG. 10. An $L = 2$ example for the $\frac{3}{2}^+[402]$ state with a (268 keV)$d$-$\theta_d$-$\gamma$(163 keV) double gate.

### B. 1296-keV level

The primary result of the present study, the reinterpretation of a level at ∼1296 keV, follows from the 1027-keV $\gamma$-gated deuteron spectrum shown in Fig. 12; this $\gamma$ ray has not been seen before. The deuteron peak corresponds to a measured excitation energy of 1290 ± 7 keV (cf. 1295 ± 5 keV reported by Tjøm and Elbek [5] from $(d, t)^{155}$Gd). Indeed, this is the same state seen in coincidence with the 163-keV $\gamma$ ray from the 268-keV, $\frac{3}{2}^+[402]$, level (i.e., the second deuteron peak at 1304 ± 7 keV in Fig. 9); the two gates are overlaid in Fig. 13 (and are confirmed separately by the $d$-$\gamma$-$\gamma$ coincidence data).

TABLE I. The optical model parameters [39–41] used for the proton and deuteron channels.

| Ch. | $V$ | $r_v$ | $a_v$ | $W_D$ | $r_D$ | $a_D$ | $V_s$ | $r_s$ | $a_s$ | $r_C$ | Ref. |
|---|---|---|---|---|---|---|---|---|---|---|---|
| $p$ | 55.7 | 1.20 | 0.70 | 11.3 | 1.25 | 0.70 | 12.0 | 1.10 | 0.70 | 1.20 | [39,40] |
| $d$ | 105.4 | 1.15 | 0.81 | 18.9 | 1.34 | 0.68 | ⊘ | ⊘ | ⊘ | 1.15 | [41] |

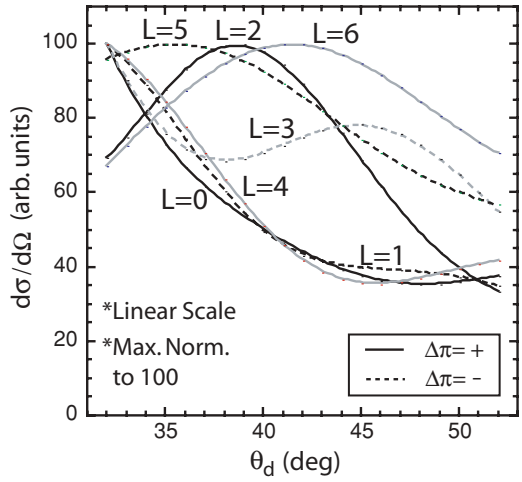


FIG. 11. A summary of angular distribution shapes using the optical model parameters in Table I.

Inspection of the total deuteron-selected 1027-keV $\gamma$ gate from $^{156}$Gd$(p, d\text{-}\gamma\text{-}\gamma)^{155}$Gd reveals that the ~1027-keV $\gamma$ ray is actually a doublet, as shown in Fig. 14. Both members of the doublet, however, originate from the same state and decay to two closely spaced low-lying states in $^{155}$Gd: a $1027.37 \pm 0.23$-keV $\gamma$ transition to the $\frac{3}{2}^+[402]$ state at $268.6233 \pm 0.0007$ keV [4] and a $1029.54 \pm 0.31$-keV $\gamma$ transition to the $\frac{5}{2}^+[642]$ state at $266.6471 \pm 0.0007$ keV [4]. The doublet energies were resolved by gating below on well-resolved transitions that depopulate the 268- and 266-keV levels, respectively. The resulting excitation energies are thus $1295.99 \pm 0.23$ and $1296.19 \pm 0.31$ keV, respectively, which correspond to the same level.

A total of twelve new $\gamma$-ray decays are found that depopulate the 1296-keV level. The measured (linear-weighted average) excitation energy is found to be

$$E_x^d = 1293 \pm 6 \text{ keV}$$

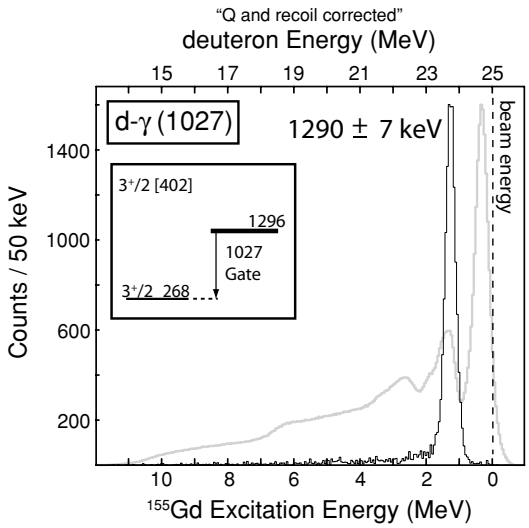


FIG. 12. The deuteron spectrum in coincidence with the 1027-keV $\gamma$ ray (black).

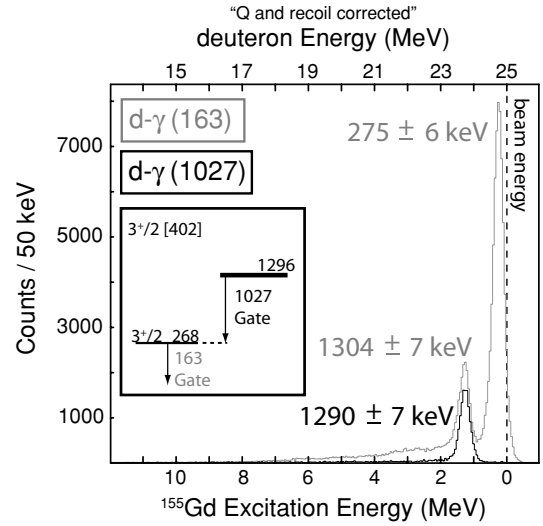


FIG. 13. The deuteron spectrum in coincidence with the 1027-keV $\gamma$ ray (black) and the deuteron spectrum in coincidence with the 163-keV $\gamma$ ray (gray).

from the deuterons [see Fig. 15(a)] and

$$E_x = 1296.13 \pm 0.11 \text{ keV}$$

from the $\gamma$-ray energies [see Fig. 15(b)]. The excitation versus $\gamma$-ray energy points in Fig. 15(b) with circles are confirmed by the $d\text{-}\gamma\text{-}\gamma$ coincidence data. A particular advantage of having the excitation energy measured by the deuterons is that it can highlight "missing" transitions, which could be overlooked by use of $\gamma$ rays alone. Figure 15 indicates the power and consistency of the present particle-$\gamma$ method in establishing level energies.

The decay scheme for the 1296-keV level is shown in Fig. 16 with a spin and parity assignment of $J^\pi = \frac{5}{2}^+$. This is in contradiction with the current literature [4]. Tjøm and Elbek [5] report a level at $1295 \pm 5$ keV for $(d, t)^{155}$Gd in a systematic study of $^{151-161}$Gd by $(d, p)$ and $(d, t)$; this is likely the same level seen in the present single-neutron transfer study. However, they report an angular momentum transfer value of $L = 4$ and establish it as the $\frac{7}{2}^+[404]$ state. This was assigned for two reasons: (a) The angular distribution was consistent with a $L = 4$ distribution, which was systematically applied based on their $(d, t)^{159}$Gd results (although, they do note that the absolute intensity was larger than expected) and (b) the $\frac{7}{2}^+[404]$ orbital was expected to be the next hole state for $L = 4$ transfer. This assignment was further asserted in a follow-up $(d, t)^{155}$Gd study of theirs led by Jaskola [8]. A level at $1297 \pm 15$ keV is also reported by Løvhøiden and co-workers [12] in $(^3\text{He}, \alpha)^{155}$Gd, where $\langle L \rangle = 4\hbar$–$6\hbar$. Whereas they seem to claim that they cannot distinguish between $L = 2$ and 4, they adopt the $L = 4$, $\frac{7}{2}^+[404]$ assignment but state that the observed intensity is a factor of 2 or 3 lower than theory.

Schmidt *et al.* [15] repeat the $(d, t)$ and $(d, p)$ study of Tjøm and Elbek [5] but also include a $(n, \gamma)^{155}$Gd study, which provides essentially all of the $\gamma$-ray data for $E > 750$ keV in the NDS [4]. The other $\gamma$-ray studies were done by $\beta$ decay

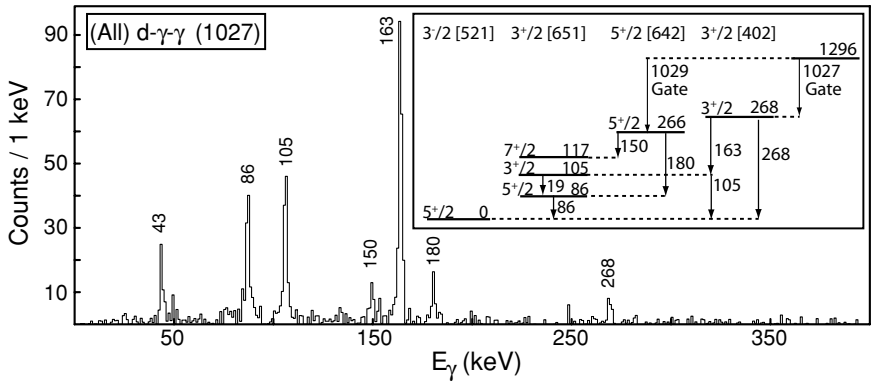


FIG. 14. The total deuteron-selected 1027-keV $\gamma$ gate from $d$-$\gamma$-$\gamma$.

that fed states below 750 keV (e.g., Meyer *et al.* [14]) or they were done with reactions that preferentially populated collective and/or high-spin states. Schmidt *et al.* [15] report a $L = 0$–5 state at $1297.24 \pm 0.18$ keV from the average of their $(d, p)$ and $(d, t)$ results (although we question their reported energy and error; see the following). They also report a level at $1297.181 \pm 0.012$ keV from use of secondary $\gamma$ rays in the $(n, \gamma)^{155}$Gd reaction (and note that this energy was then used to iteratively calibrate their particle energy). No spin assignment was made from primary $\gamma$ decay but they adopt $J^\pi = \frac{5}{2}^+, \frac{7}{2}^+$ from secondary $\gamma$ rays and give the following branches (not normalized to level): $I_\gamma(1150.4\ \text{keV}) = 62 \pm 5$, $I_\gamma(808.4\ \text{keV}) = 33 \pm 5$, $I_\gamma(192.4\ \text{keV}) = 2.1 \pm 0.5$, and $I_\gamma(104.3\ \text{keV}) = 3.7 \pm 0.9$. The first two branches reported by Schmidt *et al.* [15], $I_\gamma(1150.4\ \text{keV})/I_\gamma(808.4\ \text{keV}) \sim 1.9$, are not the same as those found in the present study, $I_\gamma(1150.09 \pm 0.24\ \text{keV})/I_\gamma(807.29 \pm 0.12\ \text{keV}) \sim 0.4$. Furthermore, the strongest $\gamma$ branch is presently found to be $1027.37 \pm 0.23$ keV and/or the ~1027-keV doublet, which is not mentioned at all by Schmidt *et al.* [15]. Therefore, the $1297.181 \pm 0.012$-keV state and $\gamma$ branches from their $(n, \gamma)^{155}$Gd study were incorrectly associated with the nearly degenerate level seen in their single-neutron transfer data, $(d, t)$ and $(d, p)$. Indeed, the present particle-$\gamma$ coincidence technique avoids these kind of mistakes between multiple experiments.

Our present $J^\pi = \frac{5}{2}^+$ assignment (cf. Fig. 16) for the 1296-keV level is supported by the $(p, d$-$\gamma)^{155}$Gd data with the following information: (a) the $L$ transfer value from the deuteron angular distribution and (b) the $\gamma$-decay paths. These are illustrated in the following.

The experimental and DWBA [38] angular distributions for the direct population of the 1296-keV level are shown in Fig. 17 by a (1296 keV)$d$-$\theta_d$-$\gamma$(1027 keV) double gate. The experimental angular distribution is most accurately described by $L = 2$ in the $\chi^2$ minimization. Anisotropy effects on the distribution shape are checked (Fig. 18) by comparing gates, (1296 keV)$d$-$\theta_d$-$\gamma$(1027 keV), for $\gamma$ rays emitted in and out of the reaction plane. There are negligible differences and both are consistent with $L = 2$. Gates on the other transitions (cf. Fig. 16) are also consistent with an $L = 2$ assignment (but with poorer statistics). Therefore, a spin and parity

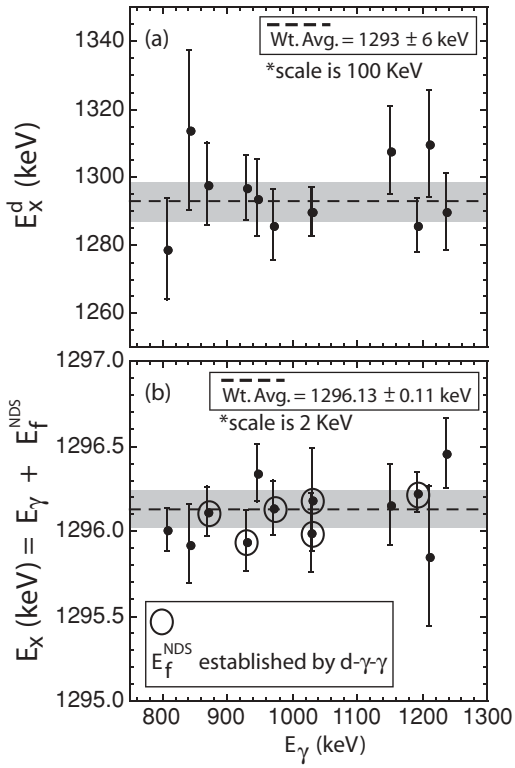


FIG. 15. The calculation of the 1296-keV level energy from deuteron and $\gamma$-ray energies.

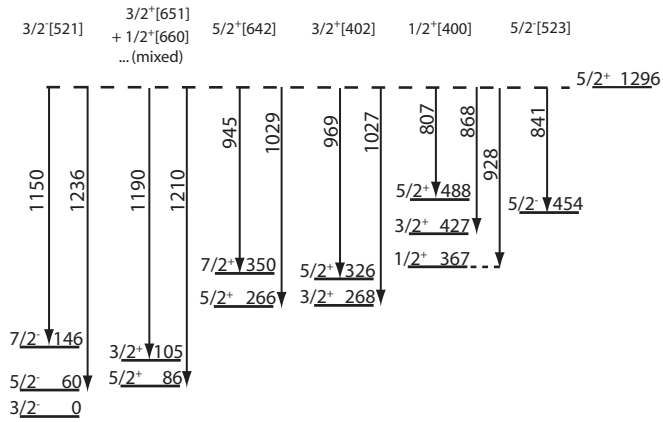


FIG. 16. A decay scheme for the 1296-keV level in $^{155}$Gd.

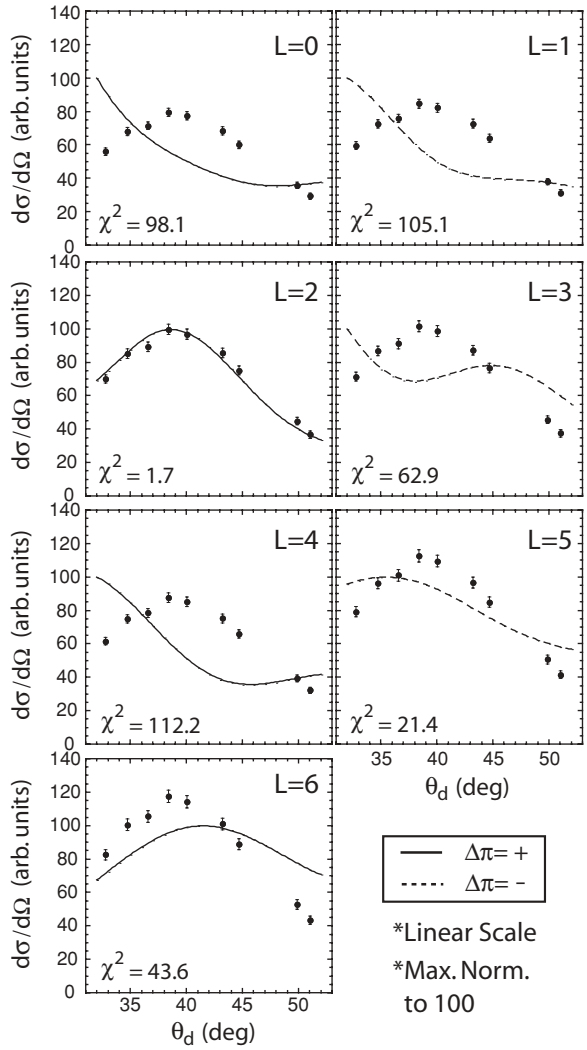


FIG. 17. An $L = 2$ transfer assignment is shown to be most favorable for the 1296-keV state with a (1296 keV)$d$-$\theta_d$-$\gamma$(1027 keV) double gate.

assignment of $J^\pi = \frac{3}{2}^+$ or $\frac{5}{2}^+$ can be made from the deuteron angular distribution. Recall that the $L = 2$ distribution was well described for the $\frac{3}{2}^+$[402] state in Fig. 10.

The previous $\frac{7}{2}^+$ assignment [4,5] is further eliminated by the observation of a 928.31 ± 0.18-keV $\gamma$ transition (cf. Fig. 16) to the 367-keV, $\frac{1}{2}^+$[400], level; a $\frac{7}{2}^+$ assignment would require an $E4$ or $M3$ decay, which are not likely. The 928-keV $\gamma$ peak is shown in Fig. 19(a) by the total deuteron-selected 262-keV $\gamma$ gate from $^{156}$Gd($p$, $d$-$\gamma$-$\gamma$)$^{155}$Gd or (all)$d$-$\gamma$-$\gamma$(262 keV) in shorthand notation. The selectivity of $d$-$\gamma$-$\gamma$ is illustrated in Fig. 19(b) by a (1296 keV)$d$-$\gamma$-$\gamma$(262 keV) double gate. The additional selectivity acquired by gating on the excitation energy (deuteron) is evident in the suppressed background and prominence of the 928-keV $\gamma$ peak.

The $\frac{3}{2}^+$ assignment is ruled out for the 1296-keV level by the observation of a 1150.09 ± 0.24-keV $\gamma$ transition (cf. Fig. 16) to the $\frac{7}{2}^-$, $\frac{3}{2}^-$[521] state at 146 keV [4]; a $\frac{3}{2}^+$ assignment would require an $E3$ or $M4$ decay, which are not likely. However, the statistics do not allow for a confirmation of the 1150-keV $\gamma$ transition by $d$-$\gamma$-$\gamma$.

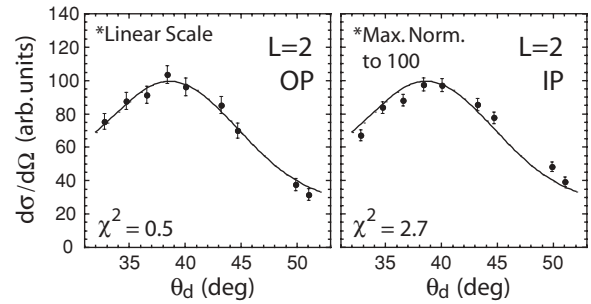


FIG. 18. An $L = 2$ transfer assignment is shown to be most probable for the 1296-keV state with a (1296 keV)$d$-$\theta_d$-$\gamma$(1027 keV) double gate. This is shown for both in-plane and out-of-plane ($p$, $d$-$\gamma$) events.

The 1296-keV state is determined to have a relative cross section of

$$\sigma(1296.13\ \text{keV}) \geqslant 34.6 \pm 1.0\ \text{(arb. units)}$$

(where $\geqslant$ signifies the fact that not all the transitions from the state may be accounted for in the present study). The $\frac{5}{2}^+$[402] orbital, which originates from the $2d_{5/2}$ spherical state, is expected to be the next $L = 2$, $J^\pi = \frac{5}{2}^+$ hole state (cf. the adopted levels and assignments in Fig. 4 and the remaining orbitals in the Nilsson diagram, Fig. 5) and it has a large $(C_{jl})^2 = 0.896$ coefficient [37]. Therefore, the 1296-keV state is assigned as the $\frac{5}{2}^+$[402] orbital.

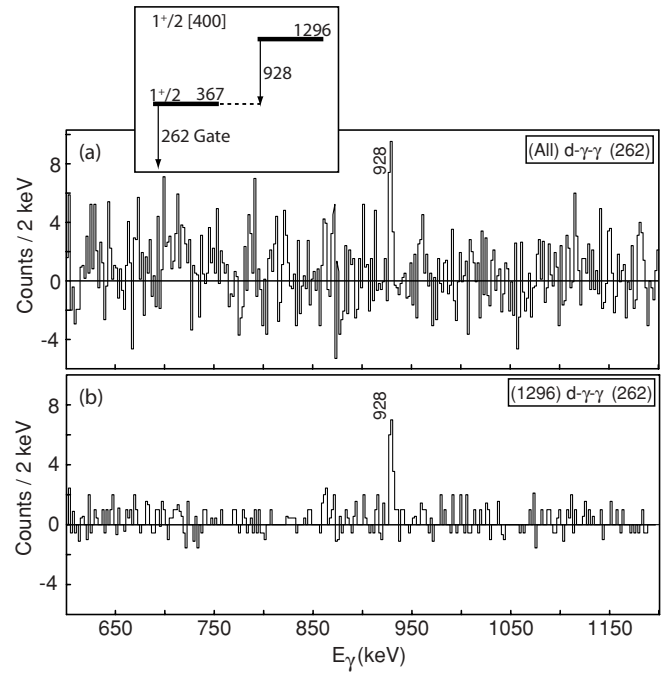


FIG. 19. The total deuteron-selected 262-keV $\gamma$ gate from $d$-$\gamma$-$\gamma$. The 262-keV $\gamma$ gate shows a coincident 928-keV $\gamma$ ray, which suggests that the 1296-keV state is $J^\pi \neq \frac{7}{2}^+$.

The present $\frac{5}{2}^+[402]$ assignment in $^{155}$Gd may indicate a larger problem with current $\frac{7}{2}^+[404]$ assignments in the rare-earth region [especially those made by $(d,t)$ studies]; there are several experimental and theoretical studies that support this. The best example that supports the present assignment comes from a neighboring $N = 91$ isotone study of $(p,d)^{153}$Sm by Blasi *et al.* [16]. They refute the $^{153}$Sm $\frac{7}{2}^+[404]$ assignment at 1532 keV that was based on the $(d,t)^{153}$Sm study by Kanestrøm and Tjøm [42] (where the $\frac{7}{2}^+[404]$ assignment was based on similarities with the $(d,t)$ systematic study of gadolinium by Tjøm and Elbek [5]). Instead, Blasi *et al.* [16] report $L = 2$ for the 1532-keV state and propose it as the $\frac{5}{2}^+[402]$ orbital. Interestingly, Blasi *et al.* [16] used a $(p,d)$ direct reaction and DWUCK4 [38] in the DWBA analysis (as does the present study). A $(^3\mathrm{He},\alpha)^{153}$Sm study [17] also reports $L = 2$ for the 1532-keV state. An $L = 2$, $J^\pi = \frac{5}{2}^+$ assignment has since been adopted by the NDS [43] for the 1532-keV state in $^{153}$Sm.

A $(p,d)^{157}$Gd study by Yagi *et al.* [44] reports no $L = 4$ state at 1825 keV, which was assigned as the $\frac{7}{2}^+[404]$ orbital in the Tjøm and Elbek systematic study [5]. However, preliminary analysis of $(p,d\text{-}\gamma)^{157}$Gd data, also taken with STARS-LIBERACE [45,46], shows a state directly populated by $L = 2$ at ~1824 keV (cf. 1825 ± 5 keV in NDS [47]). The state is observed to decay for the first time by a new ~1389-keV $\gamma$ transition [46] to the $\frac{5}{2}^-[523]$ state at 434.4 keV [47] (confirmed by $d$-$\gamma$-$\gamma$). The ~1824-keV state in $^{157}$Gd is likely to be $\frac{5}{2}^+[402]$ as well. More details will be reported on this in a future publication [46].

Several studies have reported "anomalous" $(d,t)$ angular distributions for rare-earth nuclei that have included states with $\frac{7}{2}^+[404]$ assignments [48–52]. Furthermore, these anomalous distributions are shown to persist for all beam energies [52]. Ascuitto *et al.* [53] show that the "anomalous" $(d,t)$ distributions for the yrast band are fixed by using the coupled-channel Born approximation. However, two studies by Peng *et al.* [54,55] show that coupled-channel calculations [56] do not rectify the "anomalous" distributions for nonyrast excited states nor do they provide any significant improvements over the DWBA calculations [38]. In light of the present results, previous $\frac{7}{2}^+[404]$ assignments made by $(d,t)$ studies in the gadolinium and neighboring nuclei should be reevaluated. Indeed, many may actually be $\frac{5}{2}^+[402]$.

The spectroscopic information for the "example" and "new" results are given in Table II, which organizes the data as follows: (1) $E_x$, the adopted excitation energy of the level, (2) $E_\gamma$, the $\gamma$-ray energy depopulating the level, (3) $I_\gamma$, the $\gamma$-ray peak intensity (normalized to the strongest decay branch of the level), (4) $E_x^d$, the excitation energy of the level measured by the deuterons, (5) $E_x^d - E_\gamma$, the final level energy, $E_f$, after $\gamma$ decay, (6) $E_f^{\mathrm{NDS}}$, the adopted final level energy [4], (7) $J_f^\pi$,$\Omega_f^\pi[Nn_z\Lambda]$, the adopted spin and Nilsson assignment of the final level energy [4], (8) $d$-$\gamma$-$\gamma$, the use of triple coincidences in confirming decay paths, (9) $E_\gamma + E_f^{\mathrm{NDS}}$, the excitation energy, $E_x$, measured by the $\gamma$ rays, (10) $L$, the present angular momentum transfer assignment, (11) $J^\pi$, the present spin assignment, and (12) $J^{\pi,\mathrm{NDS}}$, the NDS [4] spin assignment.

The relative cross sections and Nilsson assignments are given in Table III for the example and new results but also for the established states, NDS [4], that can be measured by at least a single $\gamma$ branch; those that cannot be measured are listed for completeness only if they pertain to a notable level. The $C_{jl}$ (Nilsson) expansion coefficients of Chi [37] are also given along with calculated occupancies, $V^2$ (based on the experimental energies, which could have a few hundred keV of rotational energy necessarily included). Recall that the quantities $C_{jl}^2$ and $V^2$ are directly proportional to the expected cross section [cf. Eq. (3)] and, therefore, provide a simple means for establishing (qualitatively) any remaining Nilsson assignments [4].

As can be seen from the tabulated relative cross sections in Table III, the 1296-keV, $\frac{5}{2}^+[402]$, level is the third largest positive-parity cross section in $(p,d)^{155}$Gd. Therefore, the $\nu\,\frac{1}{2}^+[400]$, $\nu\,\frac{3}{2}^+[402]$, and $\nu\,\frac{5}{2}^+[402]$ orbitals, which originate from the $3s_{1/2}$, $2d_{3/2}$, and $2d_{5/2}$ spherical states, respectively, account for the three largest positive-parity cross sections. These three steeply upsloping orbitals undergo $\Delta N = 2$ mixing with their $N = 6$ orbital partners, which are oppositely sloped with respect to deformation (cf. the Nilsson diagram in Fig. 5). The presence of these steeply sloped and crossing orbitals near the Fermi surface could weaken the monopole pairing strength and increase the quadrupole pairing strength of neighboring even-even nuclei, which would bring $\nu$ 2p-2h $0^+$ states below $2\Delta$. Indeed, this could account for a large number of the low-lying $0^+$ states populated by the $(p,t)^{154}$Gd direct reaction [23,39]; a more detailed description of this will be given in a future publication using the $(p,t\text{-}\gamma)$ results of the present experiment [57] (cf. the tritons in Fig. 2). The remaining states will be briefly discussed in the following.

### C. 592-keV level

A new level is found by two $\gamma$ decays, $474.53 \pm 0.17$ and $484.85 \pm 0.11$ keV, with coincident deuteron peaks corresponding to a linear-weighted average excitation energy of

$$E_x^d = 591 \pm 10\ \mathrm{keV}$$

from the deuterons and

$$E_x = 592.46 \pm 0.11\ \mathrm{keV}$$

from the $\gamma$-ray energies (cf. Table II). The 474-keV $\gamma$ transition decays to the $\frac{7}{2}^+$, $\frac{3}{2}^+[651]$ level at 117 keV and the 484-keV $\gamma$ transition decays to the $\frac{9}{2}^+$, $\frac{3}{2}^+[651]$ level at 107 keV. The 484-keV $\gamma$ decay to the 107-keV level is confirmed in the $d$-$\gamma$-$\gamma$ data but it is only considered "consistent" or "compatible" because the 21-keV $\gamma$ decay [4] out of the 107-keV level is not observed but the subsequent $\gamma$ decay out of the $107 - 21 = 86$-keV level by a 86-keV $\gamma$ ray is observed. From the $\gamma$-decay paths and $L = 2$ transfer assignment, the spin of the 592-keV level is determined to be $J^\pi = \frac{5}{2}^+$. Meyer *et al.* [14] do report two $\gamma$ rays with energies of $474.11 \pm 0.15$ and $484.8 \pm 0.1$ keV, but they make no level assignment.

TABLE II. Spectroscopic information from $(p, d\text{-}\gamma)^{155}$Gd for examples and new results. See text for details.

| $E_x$ (keV) | $E_\gamma$ (keV) | $I_\gamma$ [a] | $E_x^d$ (keV) | $E_x^d - E_\gamma$ (keV) | $E_f^{\rm NDS}$ (keV) | $J_f^\pi, \Omega_f^\pi[Nn_z\Lambda]$ | $d$-$\gamma$-$\gamma$ [b] | $E_\gamma + E_f^{\rm NDS}$ (keV) | $L$ | $J^\pi$ | $J^{\pi,\rm NDS}$ |
|---|---|---|---|---|---|---|---|---|---|---|---|
| | | | | | Examples | | | | | | |
| **268.67**[10] | 163.40[10] | 100.0[49] | 275[6] | 112[6] | 105.3110[6] | $\frac{3}{2}^+, \frac{3}{2}^+[651]$ | y | 268.71[10] | | | |
| | 268.64[10] | 15.73[67] | 273[7] | 4[7] | 0 | $\frac{3}{2}^-, \frac{3}{2}^-[521]$ | y | 268.64[10] | | | |
| | | | **274**[5] | | | | | **268.67**[10] | 2 | $(\frac{3}{2}^+), \frac{5}{2}^+$ | $\frac{3}{2}^+$ |
| **367.66**[10] | 262.34[10] | 100.0[16] | 364[5] | 102[5] | 105.3110[6] | $\frac{3}{2}^+, \frac{3}{2}^+[651]$ | y | 367.65[10] | | | |
| | 281.22[13] | 5.82[17] | 374[6] | 93[6] | 86.5468[6] | $\frac{5}{2}^+, \frac{3}{2}^+[651]$ | y | 367.76[13] | | | |
| | | | **367**[7] | | | | | **367.66**[10] | 0,1,5 | $(\frac{1}{2}^+), \frac{3}{2}^-$ | $\frac{1}{2}^+$ |
| | | | | | New Results | | | | | | |
| **592.46**[11] | 474.53[17] | 18.0[15] | 603[12] | 128[12] | 117.9986[7] | $\frac{7}{2}^+, \frac{3}{2}^+[651]$ | n | 592.53[17] | | | |
| | 484.85[11] | 100.0[35] | 585[8] | 100[8] | 107.5806[10] | $\frac{9}{2}^+, \frac{3}{2}^+[651]$ | c | 592.43[11] | | | |
| | | | **591**[10] | | | | | **592.46**[11] | 2 | $\frac{5}{2}^+$ | NA |
| **720.56**[10] | 615.25[10] | 100.0[118] | 711[13] | 96[13] | 105.3110[6] | $\frac{3}{2}^+, \frac{3}{2}^+[651]$ | y | 720.56[10] | | | |
| | | | **711**[13] | | | | | **720.56**[10] | 0,1,4 | $(\frac{1}{2}^+), \frac{1}{2}^-$ $\frac{3}{2}^-, \frac{7}{2}^+$ | $\frac{1}{2}^+, \frac{3}{2}^+$ $\frac{5}{2}^+$ |
| **752.46**[12] | 665.91[12] | 100.0[69] | 759[8] | 93[8] | 86.5468[6] | $\frac{5}{2}^+, \frac{3}{2}^+[651]$ | y | 752.46[12] | | | |
| | | | **759**[8] | | | | | **752.46**[12] | 0,1,4 | $\frac{1}{2}^+, \frac{3}{2}^-$ $(\frac{7}{2}^+), \frac{9}{2}^+$ | $\frac{5}{2}^+$ |
| **1296.13**[11] | 807.29[12] | 5.95[53] | 1279[15] | 472[15] | 488.7206[8] | $\frac{5}{2}^+, \frac{3}{2}^+[402]$ | n | 1296.01[12] | | | |
| | 841.45[23] | 2.01[37] | 1314[24] | 473[24] | 454.4746[10] | $\frac{5}{2}^-, \frac{5}{2}^-[523]$ | n | 1295.92[23] | | | |
| | 868.88[15] | 9.79[59] | 1298[12] | 429[12] | 427.2375[7] | $\frac{3}{2}^+, \frac{1}{2}^+[400]$ | y | 1296.12[15] | | | |
| | 928.31[18] | 10.35[70] | 1297[10] | 369[10] | 367.6340[8] | $\frac{1}{2}^+, \frac{1}{2}^+[400]$ | y | 1295.94[18] | | | |
| | 945.91[17] | 3.64[50] | 1294[11] | 348[11] | 350.4355[9] | $\frac{7}{2}^+, \frac{5}{2}^+[642]$ | n | 1296.35[17] | | | |
| | 970.05[16] | 17.11[81] | 1286[10] | 316[10] | 326.0880[8] | $\frac{5}{2}^+, \frac{3}{2}^+[402]$ | y | 1296.14[16] | | | |
| | 1027.37[23] | 100.0[22] | 1290[7] | 263[7] | 268.6233[7] | $\frac{3}{2}^+, \frac{3}{2}^+[402]$ | y | 1295.99[23] | | | |
| | 1029.54[31] | ↑[c] | 1290[7] | 260[7] | 266.6471[7] | $\frac{5}{2}^+, \frac{5}{2}^+[642]$ | y | 1296.19[31] | | | |
| | 1150.09[24] | 2.90[40] | 1308[13] | 158[13] | 146.0696[7] | $\frac{7}{2}^-, \frac{3}{2}^-[521]$ | n | 1296.16[24] | | | |
| | 1190.92[12] | 43.2[13] | 1286[8] | 95[8] | 105.3110[6] | $\frac{3}{2}^+, \frac{3}{2}^+[651]$ | y | 1296.23[12] | | | |
| | 1209.31[41] | 8.26[57] | 1310[16] | 101[16] | 86.5468[6] | $\frac{5}{2}^+, \frac{3}{2}^+[651]$ | n | 1295.86[41] | | | |
| | 1236.45[20] | 4.03[42] | 1290[11] | 54[11] | 60.0108[6] | $\frac{5}{2}^-, \frac{3}{2}^-[521]$ | n | 1296.46[20] | | | |
| | | | **1293**[6] | | | | | **1296.13**[11] | 2 | $\frac{5}{2}^+$ | $\frac{7}{2}^+$ |
| **1551.03**[12] | 1096.56[12] | 100.0[47] | 1549[7] | 452[7] | 454.4746[10] | $\frac{5}{2}^-, \frac{5}{2}^-[523]$ | y | 1551.03[12] | | | |
| | | | **1549**[7] | | | | | **1551.03**[12] | 2 | $(\frac{3}{2}^+), \frac{5}{2}^+$ | $(\frac{1}{2}^+, \frac{3}{2}^+)$ |
| **1577.93**[10] | 1363.55[12] | 97.2[54] | 1568[9] | 204[9] | 214.3511[14] | $\frac{13}{2}^+, \frac{3}{2}^+[651]$ | y | 1577.90[12] | | | |
| | 1470.38[12] | 100.0[59] | 1575[13] | 105[13] | 107.5806[10] | $\frac{9}{2}^+, \frac{3}{2}^+[651]$ | c | 1577.96[12] | | | |
| | | | **1571**[6] | | | | | **1577.93**[10] | 5 | $\frac{11}{2}^-$ | $\frac{11}{2}^-$ |

[a]Intensity normalized to 100 for the strongest observed branch.
[b]Entries are listed as y = yes, n = no, and c = consistent.
[c]The branches are with respect to $I_\gamma(1027.37) + I_\gamma(1029.54)$ (small error); $I_\gamma(1027.37)/I_\gamma(1029.54) \approx 3.7 \pm 0.6$ (large error).

The present $592.46 \pm 0.11$-keV level is a doublet with the previously known $K = 0 \otimes \frac{3}{2}^-[521]$ bandhead level at $592.1420 \pm 0.0018$ keV [4]; the $\gamma$ rays from this previously known level are only weakly observed in the present study. Indeed, finding this doublet resolves some inconsistencies in the literature. The $K = 0 \otimes \frac{3}{2}^-[521]$ assignment for the

TABLE III. Relative $(p, d)^{155}$Gd cross sections ($\theta_d \sim 33^\circ$–$51^\circ$) and Nilsson assignments. The $C^2_{jl}$ expansion coefficients of Chi [37] are also given along with calculated occupancies, $V^2$ (based on the experimental energies, which could have a few hundred keV of rotational energy necessarily included). Not all of the known levels [4] could be uniquely selected in the present experiment; notable states that could not be measured are listed but left blank. See text for details.

| $E_x$ | $J^{\pi,\mathrm{NDS}}$ | Modified | $\sigma^{\mathrm{rel}}$ | $J^\pi,\Omega^\pi[Nn_z\Lambda]^{\mathrm{NDS}}$ | Modified | $\epsilon$,$\lambda$ | $V^2(\epsilon > \lambda)$ | $V^2(\epsilon < \lambda)$ | $C^2_{jl}$ | $V^2 \times C^2_{jl}$ |
|---|---|---|---|---|---|---|---|---|---|---|
| 0.0 | $\frac{3}{2}^-$ | | | $\frac{3}{2}^-,\frac{3}{2}^-[521]$ | | = | 0.500 | 0.500 | 0.104 | 0.052 |
| 86.5468 [6] [a] | $\frac{5}{2}^+$ | | | $\frac{5}{2}^+,\frac{3}{2}^+[651]$ | | < | 0.460 | 0.540 | 0.080 | 0.043 |
| 105.3110 [6] [a] | $\frac{3}{2}^+$ | | | $\frac{3}{2}^+,\frac{3}{2}^+[651]$ | | < | 0.452 | 0.548 | 0.001 | 0.001 |
| 121.05 [19] [a] | $\frac{11}{2}^-$ | | | $\frac{11}{2}^-,\frac{11}{2}^-[505]$ | | > | 0.445 | 0.555 | 1.000 | 0.445 |
| 266.6471 [7] [a] | $\frac{5}{2}^+$ | | | $\frac{5}{2}^+,\frac{5}{2}^+[642]$ | | > | 0.381 | 0.619 | 0.004 | 0.002 |
| 268.67 [10] | $\frac{3}{2}^+$ | | 66.6 [32] | $\frac{3}{2}^+,\frac{3}{2}^+[402]$ | | < | 0.380 | 0.620 | 0.850 | 0.527 |
| 287.0039 [7] [a] | $\frac{3}{2}^-$ | | | $\frac{3}{2}^-,\frac{3}{2}^-[532]$ | | < | 0.372 | 0.628 | 0.038 | 0.024 |
| 321.52 [10] | $\frac{5}{2}^-$ | | 12.1 [12] | $\frac{5}{2}^-,\frac{3}{2}^-[532]$ | | < | 0.358 | 0.642 | 0.212 | 0.136 |
| 326.10 [11] | $\frac{5}{2}^+$ | | 3.32 [32] | $\frac{5}{2}^+,\frac{3}{2}^+[402]$ | | < | 0.356 | 0.644 | 0.069 | 0.045 |
| 367.66 [10] | $\frac{1}{2}^+$ | | 100.0 [27] | $\frac{1}{2}^+,\frac{1}{2}^+[400]$ | | < | 0.340 | 0.660 | 0.606 | 0.400 |
| 427.15 [11] | $\frac{3}{2}^+$ | | 15.3 [2] | $\frac{3}{2}^+,\frac{1}{2}^+[400]$ | | < | 0.317 | 0.683 | 0.237 | 0.162 |
| 450.66 [11] | $\frac{3}{2}^-$ | | 46.4 [21] | $\frac{3}{2}^-,\frac{1}{2}^-[530]$ | | < | 0.309 | 0.691 | 0.213 | 0.147 |
| 451.3714 [8] [a] | $\frac{1}{2}^-$ | | 15.7 [12] | $\frac{1}{2}^-,\frac{1}{2}^-[530]$ | | < | 0.308 | 0.692 | 0.006 | 0.004 |
| 454.4746 [10] [a] | $\frac{5}{2}^-$ | | | $\frac{5}{2}^-,\frac{5}{2}^-[523]$ | | > | 0.307 | 0.693 | 0.074 | 0.023 |
| 488.87 [16] | $\frac{5}{2}^+$ | | 14.9 [22] | $\frac{5}{2}^+,\frac{1}{2}^+[400]$ | | < | 0.295 | 0.705 | 0.112 | 0.079 |
| 553.37 [10] | $(\frac{7}{2}^-)$ | | 4.03 [18] | $\frac{7}{2}^-,\frac{3}{2}^-[532]$ | | < | 0.273 | 0.727 | 0.081 | 0.059 |
| 559.35 [10] | $\frac{1}{2}^-$ | | 2.43 [28] | $\frac{1}{2}^-,\frac{1}{2}^-[521]$ | | > | 0.271 | 0.729 | 0.249 | 0.068 |
| 592.46 [11] | NA | $\frac{5}{2}^+$ | $\geqslant$ 3.52 [13] | NA | $\frac{5}{2}^+,\frac{1}{2}^+[651]$ | > | 0.261 | 0.739 | 0.167 | 0.044 |
| 614.72 [12] | $\frac{3}{2}^-$ | | 3.09 [14] | $\frac{3}{2}^-,\frac{1}{2}^-[521]$ | | > | 0.254 | 0.746 | 0.024 | 0.006 |
| 720.56 [10] | $\frac{1}{2}^+,\frac{3}{2}^+,\frac{5}{2}^+$ | $(\frac{1}{2}^+)$ | 2.56 [31] | NA | $\frac{1}{2}^+,\frac{1}{2}^+[660]$ | < | 0.224 | 0.776 | 0.006 | 0.005 |
| 752.46 [12] | $\frac{5}{2}^+$ | $(\frac{7}{2}^+)$ | 4.30 [47] | NA | $\frac{7}{2}^+,\frac{7}{2}^+[404]$ | < | 0.216 | 0.784 | 0.982 | 0.770 |
| 1296.13 [11] | $\frac{7}{2}^+$ | $\frac{5}{2}^+$ | $\geqslant$ 34.6 [10] | $\frac{7}{2}^+,\frac{7}{2}^+[404]$ | $\frac{5}{2}^+,\frac{5}{2}^+[402]$ | < | 0.117 | 0.883 | 0.896 | 0.791 |
| 1551.03 [12] | $(\frac{1}{2}^+,\frac{3}{2}^+)$ | $(\frac{3}{2}^+)$ | $\geqslant$ 3.53 [20] | NA | $\frac{3}{2}^+,\frac{1}{2}^+[411]$ | < | 0.091 | 0.909 | 0.420 | 0.382 |
| 1577.93 [10] | $\frac{11}{2}^-$ | | $\geqslant$ 4.90 [21] | $\frac{11}{2}^-,\frac{9}{2}^-[514]$ | | < | 0.088 | 0.912 | 0.989 | 0.902 |

[a]Energy from NDS [4].

592.1420 ± 0.0018-keV level [4] is well established from several studies: (a) With two-neutron transfer, $(p, t)$, Løvhøiden *et al.* [13] show that it is populated by $L = 0$ with the second largest cross section (the ground having the largest; note that $^{157}$Gd and $^{155}$Gd both have $\frac{3}{2}^-$ ground states), (b) with inelastic scattering, $(d, d')$, Sterba *et al.* [11] show a strong population, and (c) with $^{155}$Tb $\beta$ decay, Meyer *et al.* [14] show large $E0$ admixtures in the transition to the ground state. However, Schmidt *et al.* [15] report a state populated by $L = 2$–4 at 592.57 ± 0.15 keV in their $(d, p)$ and $(d, t)$ single-neutron transfer data (cf. 592.46 ± 0.11 keV in the present study) and a $J = \frac{1}{2}^-$ or $\frac{3}{2}^-$ state at 592.1429 ± 0.0022 keV in their $(n, \gamma)$ data. They make a comment that this inconsistency could be due to a doublet. We show that this is indeed the case.

The new 592-keV state is determined to have a relative cross section of

$$\sigma(592.46\ \mathrm{keV}) \geqslant 3.52 \pm 0.13\ (\mathrm{arb.\ units})$$

(cf. Table III). The $\frac{1}{2}^+[660]$ and $\frac{1}{2}^+[651]$ neutron orbitals are the only remaining options (i.e., near the Fermi surface and above the $\frac{5}{2}^+[402]$ orbital, cf. Fig. 5) that support a $J^\pi = \frac{5}{2}^+$ spin. The $\frac{5}{2}^+$, $\frac{1}{2}^+[660]$ state has a $(C_{jl})^2 = 0.054$ coefficient and the $\frac{5}{2}^+$, $\frac{1}{2}^+[651]$ state has a $(C_{jl})^2 = 0.167$ coefficient [37]. Therefore, the $\frac{5}{2}^+$, $\frac{1}{2}^+[651]$ orbital is assigned to the 592.46 ± 0.11 keV level. Note that the cross section and $(C_{jl})^2$ coefficient for this $J^\pi = \frac{5}{2}^+$ state in Table III is much smaller than that for the $\frac{5}{2}^+[402]$ orbital at 1296 keV.

### D. 720-keV level

A 615.25 ± 0.10-keV $\gamma$ ray is found with a coincident deuteron peak corresponding to an excitation energy of

$$E^d_x = 711 \pm 13\ \mathrm{keV}$$

from the deuterons and

$$E_x = 720.56 \pm 0.10 \text{ keV}$$

from the $\gamma$-ray energy (cf. Table II). The 615-keV $\gamma$ transition decays to the $\frac{3}{2}^+$, $\frac{3}{2}^+$ [651] level at 105 keV. The decay path is confirmed with the $d$-$\gamma$-$\gamma$ coincidence data. From the $\gamma$-decay path and $L = 0,1,4$ transfer assignment, the spin of the level is determined to be $J^\pi = \frac{1}{2}^+, \frac{1}{2}^-, \frac{3}{2}^-, \frac{7}{2}^+$.

The 720-keV level was reported previously by Schmidt *et al.* [15]. They report a level at $720.50 \pm 0.24$ keV from their $(d,t)$ study and $720.6177 \pm 0.0017$ keV from secondary $\gamma$ rays in their $(n,\gamma)$ study. Indeed, they show the 615-keV $\gamma$ ray as the strongest branch. No $L$ transfer value from $(d,t)$ is reported for the level but they assign a spin of $J^\pi = \frac{1}{2}^+, \frac{3}{2}^+, \frac{5}{2}^+$ from primary $\gamma$ rays following resonance-average neutron capture. Furthermore, they assign the $\frac{1}{2}^+[660]$ orbital to this level.

Although the 720-keV level and 615-keV $\gamma$ decay are not new [15], the purpose of giving them here is to help clear confusion in the NDS [4], which has two neighboring levels at $720.6168 \pm 0.0017$ keV and 721.0 keV (no error given). The first of these, the 720-keV level, is given by Schmidt *et al.* [15] in their $(d,t)$ and $(n,\gamma)$ study, which was just mentioned earlier. The second, the 721-keV level, is given by Tveter *et al.* [9] in a Coulomb excitation study with a single $\gamma$ decay of 721.0 keV (no error given) to the ground state, $\frac{3}{2}^-[521]$; this $\gamma$ decay is not seen in the present study. Levels at $729 \pm 4$ and $725 \pm 2$ keV have also been reported by Løvhøiden *et al.* [13] with $(p,t)$ and by Sterba *et al.* [11] with $(d,d')$; these are associated with the 721-keV level from the Coulex study of Tveter *et al.* [9]. Based on these studies, the 721-keV level has been interpreted as the $J^\pi = \frac{7}{2}^-$ member of the $K = 0 \otimes \frac{3}{2}^-[521]$ bandhead at $592.1420 \pm 0.0018$ keV [4]. Curiously, Tjøm and Elbek [5] report a level at $721 \pm 3$ keV populated by $L = 3$ in their $(d,t)$ study and also interpret the level as the $J^\pi = \frac{7}{2}^-$ member of the $K = 0 \otimes \frac{3}{2}^-[521]$ band. However, a follow-up $(d,t)$ study by Jaskola *et al.* [8] claims that the angular distribution is weakly supportive of this assignment.

In the present $(p, d$-$\gamma)$ study, the measured level at $720.56 \pm 0.10$ keV and $\gamma$ decay of $615.25 \pm 0.10$ keV is consistent with the level reported by Schmidt *et al.* [15] in their $(d,t)$ and $(n,\gamma)$ study. Furthermore, the 615-keV $\gamma$ decay to the $\frac{3}{2}^+$, $\frac{3}{2}^+[651]$ level at 105 keV eliminates the possibility that the state seen in the present single-neutron transfer reaction is the $J^\pi = \frac{7}{2}^-$ member of the $K = 0 \otimes \frac{3}{2}^-[521]$ band. Therefore, the $\gamma$ branches of the 720-keV level reported by Schmidt *et al.* [15] are adopted. Because population of the 720-keV level by $L = 2$ transfer has been eliminated in the present study (i.e., $L = 0,1,4$), $J^\pi = \frac{1}{2}^+$ is the only remaining spin that is compatible with the Schmidt *et al.* [15] study.

The $720.56 \pm 0.10$-keV state is determined to have a relative cross section of

$$\sigma(720.56 \text{ keV}) = 2.56 \pm 0.31 \text{ (arb. units)}$$

(cf. Table III). The $L = 0$ and $J^\pi = \frac{1}{2}^+$ assignment makes the 720-keV level the second $J^\pi = \frac{1}{2}^+$ state in $^{155}$Gd, which is expected to be the $\frac{1}{2}^+[660]$ orbital. Furthermore, as mentioned earlier, the expected cross section to the $\frac{1}{2}^+[660]$ orbital is small. Recall that the $(C_{jl})^2$ coefficients for the $\frac{1}{2}^+[660]$ and $\frac{1}{2}^+[400]$ orbitals are 0.006 and 0.606, respectively, and they have nearly the same occupancy ($V^2 = 0.776$ and 0.660, respectively). Without mixing, the relative cross section of the $\frac{1}{2}^+[660]$ or 720-keV state would be $\approx 100 \times (0.006/0.606) \times (0.776/0.660) = 1.16$ (arb. units). The relative cross section of $2.56 \pm 0.31$ (arb. units) reveals the influence of mixing. Furthermore, the present assignment is consistent with the analogous $\frac{1}{2}^+[660]$ state at 734 keV [16,42] in the $N = 91$ isotone, $^{153}$Sm.

### E. 752-keV level

A $665.91 \pm 0.12$-keV $\gamma$ ray is found with a coincident deuteron peak corresponding to an excitation energy of

$$E_x^d = 759 \pm 8 \text{ keV}$$

from the deuterons and

$$E_x = 752.46 \pm 0.12 \text{ keV}$$

from the $\gamma$-ray energy (cf. Table II). The 665-keV $\gamma$ transition decays to the $\frac{3}{2}^+$, $\frac{3}{2}^+[651]$ level at 105 keV. The decay path is confirmed with the $d$-$\gamma$-$\gamma$ coincidence data. From the $\gamma$-decay path and $L = 0,1,4$ transfer assignment, the spin of the level is determined to be $J^\pi = \frac{1}{2}^+, \frac{3}{2}^-, \frac{7}{2}^+, \frac{9}{2}^+$.

The 752-keV level was reported previously by Schmidt *et al.* [15]. They report a level at $752.67 \pm 0.18$ keV from their $(d,t)$ and $(d,p)$ study and $752.551 \pm 0.004$ keV from secondary $\gamma$ rays in their $(n,\gamma)$ study. Indeed, they show the 665-keV $\gamma$ ray but as the second strongest branch. A 634-keV $\gamma$ transition is reported as the strongest $\gamma$ branch. Indeed, a strong 634-keV $\gamma$ decay is seen in the present study. However, they report the 634-keV $\gamma$ ray as a doublet with a decay from the 720-keV level; if there is indeed a doublet, we cannot separate it in the present study from gating above or below. Whereas Schmidt *et al.* [15] give $L = 0,1,4$ for the $(d,t)$ and $(d,p)$ reactions (Jaskola *et al.* [8] report $L = 1,3$), they adopt $J^\pi = \frac{5}{2}^+$ from the $\gamma$ decay paths, which is inconsistent with the $(d,t)$ and $(d,p)$ single-neutron transfer studies. Particularly, they report a weak $\gamma$ decay of 752 keV to the ground state, $\frac{3}{2}^-[521]$, and two $M1/E2$ $\gamma$ decays of 665 and 329 keV to states of spin $\frac{5}{2}^+$ and $\frac{7}{2}^+$, respectively. However, despite the 752-keV $\gamma$-ray energy being equivalent to the level energy, they report it as a secondary $\gamma$ ray and make no spin assignment based on primary $\gamma$ rays following resonance-average neutron capture. Faced with these inconsistencies, we believe that the weak 752-keV transition to the $J^\pi = \frac{3}{2}^-$ ground state, which was the basis of the $J^\pi = \frac{5}{2}^+$ assignment [15], is most likely misplaced or incorrect; recall that $L = 2$ (and hence $L \neq 2$) can be uniquely identified in the present experiment (cf. Fig. 10). If this is indeed the case, then the only compatible spin that remains between the present study and Schmidt *et al.* [15] is $J^\pi = \frac{7}{2}^+$ and, therefore, $L = 4$.

The $752.46 \pm 0.12$-keV state is determined to have a relative cross section of

$$\sigma(752.46\ \text{keV}) = 4.30 \pm 0.47\ \text{(arb. units)}$$

(cf. Table III). The largest $L = 4$, $J^\pi = \frac{7}{2}^+$ cross section is expected to be from the $\frac{7}{2}^+[404]$ orbital, which has a large $(C_{jl})^2$ coefficient of 0.982. Furthermore, the $\frac{7}{2}^+[404]$ orbital is expected to be lower in excitation energy than the $\frac{5}{2}^+[402]$ orbital (cf. the Nilsson diagram in Fig. 5), which is presently assigned to the 1296-keV level. The 752-keV level is the only observed case of $L = 4$ transfer in the present study that can be uniquely selected in the $d$-$\gamma$ coincidence data. Despite the large $(C_{jl})^2$ coefficient, the cross section for $L = 4$ is expected to be weak for the $(p, d)$ reaction (i.e., $\langle L\rangle = 0\hbar - 2\hbar$), which is consistent with the quoted relative cross section.

### F. 1551-keV level

A new $\gamma$ ray at $1096.56 \pm 0.12$ keV is found with a coincident deuteron peak corresponding to an excitation energy of

$$E_x^d = 1549 \pm 7\ \text{keV}$$

from the deuterons and

$$E_x = 1551.03 \pm 0.12\ \text{keV}$$

from the $\gamma$-ray energy (cf. Table II). The 1096-keV $\gamma$ transition decays to the $\frac{5}{2}^-$, $\frac{5}{2}^-[523]$ level at 454 keV. The decay path is confirmed with the $d$-$\gamma$-$\gamma$ coincidence data. From the $\gamma$-decay path and $L = 2$ transfer assignment, the spin of the level is determined to be $J^\pi = \frac{3}{2}^+, \frac{5}{2}^+$.

A level at $1551.7 \pm 0.4$ keV was reported in $(d, t)$ by Schmidt *et al.* [15] but they give no $L$ value for the transfer. However, they report a level at $1551.3 \pm 0.8$ keV from primary $\gamma$ rays following resonance-average neutron capture in their $(n, \gamma)$ study and assign the level to a spin of $J^\pi = \frac{1}{2}^+, \frac{3}{2}^+$ from that, although they report no specific $\gamma$-ray energy. If their 1551-keV level from $(n, \gamma)$ is indeed the same as that seen in their $(d, t)$ study and the present $(p, d$-$\gamma)$ study, then a spin of $J^\pi = \frac{3}{2}^+$ is the only compatible choice.

The $1551.03 \pm 0.12$-keV state is determined to have a relative cross section of

$$\sigma(1551.03\ \text{keV}) \geqslant 3.53 \pm 0.20\ \text{(arb. units)}$$

(cf. Table III). The $\frac{1}{2}^+[411]$ and $\frac{3}{2}^+[411]$ neutron orbitals are the only remaining options that support a $J^\pi = \frac{3}{2}^+$ spin. The $\frac{3}{2}^+$, $\frac{1}{2}^+[411]$ state has a $(C_{jl})^2 = 0.420$ coefficient and the $\frac{3}{2}^+$, $\frac{3}{2}^+[411]$ state has a $(C_{jl})^2 = 0.017$ coefficient [37]. Therefore, the $\frac{3}{2}^+$, $\frac{1}{2}^+[411]$ orbital is assigned to the $1551.03 \pm 0.12$-keV level.

### G. 1577-keV level

Two new $\gamma$ rays, at $1363.55 \pm 0.12$ and $1470.38 \pm 0.12$ keV, are found with coincident deuteron peaks corresponding to a linear-weighted average excitation energy of

$$E_x^d = 1571 \pm 6\ \text{keV}$$

from the deuterons and

$$E_x = 1577.93 \pm 0.10\ \text{keV}$$

from the $\gamma$-ray energies (cf. Table II). The 1363-keV $\gamma$ transition decays to the $\frac{13}{2}^+$, $\frac{3}{2}^+[651]$ level at 214 keV and the 1470-keV $\gamma$ transition decays to the $\frac{9}{2}^+$, $\frac{3}{2}^+[651]$ level at 107 keV. The 1363-keV $\gamma$ decay to the 214-keV level is confirmed in the $d$-$\gamma$-$\gamma$ coincidence data. The 1470-keV $\gamma$ decay to the 107-keV level is also confirmed in the $d$-$\gamma$-$\gamma$ coincidence data but it is only considered "consistent" or "compatible" because the 21-keV $\gamma$ decay [4] out of the 107-keV level is not observed but the subsequent $\gamma$ decay out of the $107 - 21 = 86$-keV level by a 86-keV $\gamma$ ray is observed. From the $\gamma$-decay paths and $L = 5$ transfer assignment, the spin of the 1577-keV level is determined to be $J^\pi = \frac{11}{2}^-$.

A level at $1581 \pm 15$ keV was reported in $(^3\text{He}, \alpha)$ by Løvhøiden *et al.* [12] with an $L = 5$ transfer assignment. The level was assigned as the $\frac{11}{2}^-$, $\frac{9}{2}^-[514]$ orbital. Indeed, this is likely the same level as seen in the present study. However, because $\gamma$ rays are measured in the present $(p, d$-$\gamma)$ study, the level energy can now be firmly established (cf. $1577.93 \pm 0.10$ versus $1581 \pm 15$ keV).

The 1577-keV state is determined to have a relative cross section of

$$\sigma(1577.93\ \text{keV}) \geqslant 4.90 \pm 0.21\ \text{(arb. units)}$$

(cf. Table III). The next $J^\pi = \frac{11}{2}^-$ state populated by $L = 5$ transfer is expected to originate from the $h_{11/2}$ spherical state. Because the $\frac{11}{2}^-[505]$ orbital has already been assigned [4] (cf. Fig. 4), $\frac{9}{2}^-[514]$ is the next expected orbital. Furthermore, the $\frac{11}{2}^-$, $\frac{9}{2}^-[514]$ state has a near-unity $(C_{jl})^2 = 0.989$ coefficient [37], which is needed to overcome the expected weak $L = 5$ transfer strength in $(p, d)$. Therefore, the $1577.93 \pm 0.10$-keV level is given the $\frac{11}{2}^-$, $\frac{9}{2}^-[514]$ assignment. Indeed, this is consistent with the assignment made by Løvhøiden *et al.* [12].

## IV. SUMMARY AND CONCLUSIONS

In summary, a new low-energy doublet state at 592.46 keV (previously associated with the $K = 0 \otimes \frac{3}{2}^-[521]$ bandhead) and several new $\gamma$-ray transitions (particularly for states >1 MeV) are reported. Most notably, the 1296-keV level has been reassigned as the $\nu\ \frac{5}{2}^+[402]$ Nilsson orbital (previously $\nu\ \frac{7}{2}^+[404]$ [4]), which brings into question the other $\nu\ \frac{7}{2}^+[404]$ assignments in the region; a preliminary analysis of $(p, d$-$\gamma)^{157}$Gd data [45,46] supports the same change. This reassignment makes the $\nu\ \frac{1}{2}^+[400]$ (367-keV), $\nu\ \frac{3}{2}^+[402]$ (268-keV), and $\nu\ \frac{5}{2}^+[402]$ (1296-keV) orbitals, which originate from the $3s_{1/2}$, $2d_{3/2}$, and $2d_{5/2}$ spherical states, respectively, responsible for the three largest cross sections to positive-parity states in the $(p, d)^{155}$Gd direct reaction. These three steeply upsloping orbitals undergo $\Delta N = 2$ mixing with

their $N = 6$ orbital partners, which are oppositely sloped with respect to deformation (cf. the Nilsson diagram in Fig. 5). The presence of these steeply sloped and crossing orbitals near the Fermi surface could weaken the monopole pairing strength and increase the quadrupole pairing strength of neighboring even-even nuclei, which would bring $\nu$ 2p-2h $0^+$ states below $2\Delta$. Indeed, this could account for a large number of the low-lying $0^+$ states populated by the $(p, t)^{154}$Gd direct reaction [23,39].

The present $^{156}$Gd$(p, d\text{-}\gamma)^{155}$Gd study reveals that particle-$\gamma$ coincidence measurements with a segmented Si telescope and HPGe array (following a direct reaction with light ions) can accurately establish quasineutron states and their $\gamma$ decays. This avoids discrepancies that sometimes occur between multiple experiments that measure particles and $\gamma$ rays separately. A systematic study of the rare-earth region (and others) by the present method could challenge and rigorously check the current Nilsson assignment systematics (particularly for excitations $>1$ MeV). With the advent of radioactive ion beam studies, it is important to correctly understand the foundation from which we extrapolate.

## ACKNOWLEDGMENTS

The authors thank the 88-Inch Cyclotron operations and facilities staff for their help in performing this experiment and P. E. Garrett, I. Y. Lee, A. O. Macchiavelli, and J. L. Wood for useful discussions related to technique and/or physics. This work was performed under the auspices of the National Science Foundation and the US Department of Energy by the University of Richmond under Grant Nos. DE-FG52-06NA26206 and DE-FG02-05ER41379, Lawrence Livermore National Laboratory under Contract Nos. W-7405-Eng-48 and DE-AC52-07NA27344, and Lawrence Berkeley National Laboratory under Contract No. DE-AC02-05CH11231.

[1] G. Scharff-Goldhaber, Phys. Rev. **90**, 587 (1953).
[2] A. Bohr and B. R. Mottelson, Phys. Rev. **90**, 717 (1953).
[3] A. Bohr and B. R. Mottelson, *Nuclear Structure*, Vol. II (Benjamin, Reading, MA, 1975).
[4] C. W. Reich, Nucl. Data Sheets **104**, 1 (2005).
[5] P. O. Tjøm and B. Elbek, Mat. Fys. Medd. K. Dan. Vidensk. Selsk. **36**, 8 (1967).
[6] C. Foin, J. Oms, and J.-L. Barat, J. Phys. (Paris) **28**, 861 (1967).
[7] R. A. Meyer and J. W. T. Meadows, Nucl. Phys. A **132**, 177 (1969).
[8] M. Jaskola, P. O. Tjøm, and B. Elbek, Nucl. Phys. A **133**, 65 (1969).
[9] A. Tveter and B. Herskind, Nucl. Phys. A **134**, 599 (1969).
[10] G. Løvhøiden, J. C. Waddington, K. A. Hagemann, S. A. Hjorth, and H. Ryde, Nucl. Phys. A **148**, 657 (1970).
[11] F. Sterba, P. O. Tjøm, and B. Elbek, Nucl. Phys. A **162**, 353 (1971).
[12] G. Løvhøiden, J. C. Waddington, C. Ellegaard, and P. O. Tjøm, Nucl. Phys. A **160**, 305 (1971).
[13] G. Løvhøiden, D. G. Burke, and J. C. Waddington, Can. J. Phys. **51**, 1369 (1973).
[14] R. A. Meyer, R. Gunnink, C. M. Lederer, and E. Brown, Phys. Rev. C **13**, 2466 (1976).
[15] H. H. Schmidt *et al.*, J. Phys. G **12**, 411 (1986).
[16] N. Blasi, S. Micheletti, M. Pignanelli, R. De Leo, A. Gollwitzer, S. Deylitz, B. D. Valnion, G. Graw, and L. A. Malov, Nucl. Phys. A **624**, 433 (1997).
[17] A. Gollwitzer *et al.*, Acta Phys. Pol. B **27**, 481 (1996); A. Gollwitzer, thesis, Ludwig-Maximilians Universität München, 1997.
[18] R. F. Casten, M. Wilhelm, E. Radermacher, N. V. Zamfir, and P. von Brentano, Phys. Rev. C **57**, R1553 (1998).
[19] N. V. Zamfir, R. F. Casten, M. A. Caprio, C. W. Beausang, R. Krücken, J. R. Novak, J. R. Cooper, G. Cata-Danil, and C. J. Barton, Phys. Rev. C **60**, 054312 (1999).
[20] W. D. Kulp *et al.*, Phys. Rev. C **71**, 041303(R) (2005).
[21] P. E. Garrett *et al.*, Phys. Rev. Lett. **103**, 062501 (2009).
[22] W. D. Kulp, J. L. Wood, K. S. Krane, J. Loats, P. Schmelzenbach, C. J. Stapels, R.-M. Larimer, and E. B. Norman, Phys. Rev. Lett. **91**, 102501 (2003).
[23] D. A. Meyer *et al.*, Phys. Rev. C **74**, 044309 (2006).
[24] S. G. Nilsson, Mat. Fys. Medd. K. Dan. Vidensk. Selsk. **29**, 16 (1955).
[25] I. Kanestrøm and G. Løvhøiden, Phys. Norv. **5**, 2 (1971).
[26] I. Kanestrøm and P. O. Tjøm, Nucl. Phys. A **145**, 461 (1970).
[27] J. Borggreen, G. Løvhøiden, and J. C. Waddington, Nucl. Phys. A **131**, 241 (1969).
[28] M. E. Bunker and C. W. Reich, Phys. Lett. B **25**, 396 (1967).
[29] B. Elbek and P. O. Tjøm, Adv. Nucl. Phys. **3**, 259 (1969).
[30] M. E. Bunker and C. W. Reich, Rev. Mod. Phys. **43**, 348 (1971).
[31] J. T. Burke *et al.*, Phys. Rev. C **73**, 054604 (2006).
[32] S. R. Lesher, L. Phair, L. A. Bernstein, D. L. Bleuel, J. T. Burke, J. A. Church, P. Fallon, J. Gibelin, N. D. Scielzo, and M. Wiedeking, Nucl. Instrum. Methods Phys. Rev. A (2010), doi:10.1016/j.nima.2010.04.017.
[33] G. Duchêne, F. A. Beck, P. J. Twin, G. de France, D. Curien, L. Hana, C. W. Beausang, M. A. Bentley, P. J. Nolan, and J. Simpson, Nucl. Instrum. Methods Phys. Res. A **432**, 90 (1999); Z. Elekes, T. Belgya, G. L. Molnár, A. Z. Kiss, M. Csatlós, J. Gulyás, A. Krasznahorkay, and Z. Máté, *ibid.* **503**, 580 (2003).
[34] S. Frauendorf, Nucl. Phys. A **677**, 115 (2000).
[35] F. Rybicki, T. Tamura, and G. R. Satchler, Nucl. Phys. A **146**, 659 (1970).
[36] G. R. Satchler, Ann. Phys. (NY) **3**, 275 (1958).
[37] B. E. Chi, Nucl. Phys. **83**, 97 (1966).
[38] P. D. Kunz, DWUCK4, University of Colorado (unpublished).
[39] D. G. Fleming, C. Günther, G. Hagemann, B. Herskind, and P. O. Tjøm, Phys. Rev. C **8**, 806 (1973).
[40] D. G. Fleming, M. Blann, H. W. Fulbright, and J. A. Robbins, Nucl. Phys. A **157**, 1 (1970).
[41] C. M. Perey and F. G. Perey, At. Data Nucl. Data Tables **17**, 1 (1976).
[42] I. Kanestrøm and P. O. Tjøm, Nucl. Phys. A **179**, 305 (1972).
[43] R. G. Helmer, Nucl. Data Sheets **107**, 507 (2006).

[44] K. Yagi, Y. Saji, Y. Ishizaki, and T. Ishimatsu, Nucl. Phys. A **138**, 133 (1969).
[45] N. D. Scielzo *et al.*, Phys. Rev. C **81**, 034608 (2010).
[46] J. M. Allmond *et al.* (to be published).
[47] R. G. Helmer, Nucl. Data Sheets **103**, 565 (2004).
[48] J. V. Maher, G. H. Wedberg, J. J. Kolata, J. C. Peng, and J. L. Ricci, Phys. Rev. C **8**, 2390 (1973).
[49] J. C. Peng, J. V. Maher, G. H. Wedberg, and C. M. Cheng, Phys. Rev. C **13**, 1451 (1976).
[50] J. V. Maher, H. S. Song, G. H. Wedberg, and J. L. Ricci, Phys. Rev. C **14**, 40 (1976).
[51] H. S. Song, J. J. Kolata, and J. V. Maher, Phys. Rev. C **16**, 1363 (1977).
[52] H. S. Song and J. V. Maher, Phys. Rev. C **18**, 714 (1978).
[53] R. J. Ascuitto, C. H. King, and L. J. McVay, Phys. Rev. Lett. **29**, 1106 (1972).
[54] J. C. Peng, H. S. Song, F. C. Wang, and J. V. Maher, Phys. Rev. Lett. **41**, 225 (1978).
[55] J. C. Peng, H. S. Song, F. C. Wang, and J. V. Maher, Nucl. Phys. A **341**, 440 (1980).
[56] P. D. Kunz, CHUCK3, University of Colorado (unpublished).
[57] J. M. Allmond *et al.* (to be published).